# DESIGN AND ANALYSIS OF A PISTON FOR COMPRESSED NATURAL GAS (CNG) ENGINE

SULAIMAN BIN ALIAS

UNIVERSITI MALAYSIA PAHANG

# DESIGN ANALYSIS OF A PISTON FOR COMPRESSED NATURAL GAS (CNG) ENGINE

SULAIMAN BIN ALIAS

A report submitted in partial fulfilment of the requirements
for the award of degree in
Bachelor of Mechanical Engineering with Automotive Engineering

Faculty of Mechanical Engineering
UNIVERSITI MALAYSIA PAHANG

NOVEMBER 2008

## SUPERVISOR'S DECLARATION

We hereby declare that we have checked this project and in our opinion this project is satisfactory in terms of scope and quality for the award of the degree of Bachelor of Mechanical Engineering with Automotive/Manufacturing*

Signature

Name of Supervisor: Prof Madya Dr Rosli Bin Abu Bakar

Position: Dean of Faculty of Mechanical Engineering

Date: 10 November 2008

Signature

Name of Co-Supervisor: Abdul Rahim Bin Ismail

Position: Lecture

Date: 10 November 2008

Signature

Name of Panel:

Position:

Date: 10 November 2008

## STUDENT'S DECLARATION

I hereby declare that the work in this thesis is my own except for quotations and summaries which have been duly acknowledged. The thesis has not been accepted for any degree and is not concurently submitted for award of other degree.

Signature

Name: SULAIMAN BIN ALIAS

ID Number: MH05067

Date: 10 November 2008

## ACKNOWLEDGEMENTS

First of all, I would like to thank my advisor Mr Abdul Rahim Bin Ismail for his assistance in completing the PSM project. For those who have assisted I on experimental work successfully, the suggestions and encourage have helped me in all time, beginning from the concept design until completing analysis piston process and in writing the report. Without his opinion and ideas it would be difficult for me to complete and success in this project. Besides that, I would like to appreciate those who gave me the possibility to complete this project. As a student, I accept all the guidance given by my advisor. During this project, I have encountered so many problems. Without them, I would not have made it through.

I would also like to acknowledge with much appreciation to the crucial role of Dean Faculty of Mechanical Engineering, Associate Prof. Dr Rosli Bin Abu Bakar, for his advice and instruction toward finishing my project. Especially to my friends who took in this project by giving great idea in designing the Piston, using Solidwork and Algor software.

I would like to thank my family for their continuous support and confidence in my effort. They inspires me for what I have achieved today most importantly, is their guidance and motivation, in order for me to become a worthy person for the religion, race and state.

## ABSTRACT

Engine pistons are one of the most complex components among all automotive or other industry field components. The engine can be called the heart of a car and the piston may be considered the most important part of an engine. There are lots of research works proposing for engine pistons, new geometries, materials and manufacturing techniques, and this evolution has undergone with a continuous improvement over the last decades and required thorough examination of the smallest details. Notwithstanding all these studies, there is huge number of damaged pistons. Damage mechanisms have different origins and are mainly wear, temperature, and fatigue related. Among the fatigue damages, thermal fatigue and mechanical fatigue, either at room or at high temperature, play a prominent role.

This work is concerned only with the analysis of fatigue-damaged pistons. Pistons from diesel engines will be analyzed. Damages initiated at the crown, ring grooves, pin holes and skirt are assessed. A compendium of case studies of fatigue-damaged pistons is presented. An analysis of both thermal fatigue and mechanical fatigue damages is presented and analyzed in this work.

A linear static stress analysis, using “Algor works”, is used to determine the stress distribution during the combustion. Stresses at the piston crown and pin holes, as well as stresses at the grooves and skirt as a function of land clearances are also presented. A fractographic study is carried out in order to confirm crack initiation sites.

# ABSTRAK

Piston enjin adalah merupakan komponen yang complex di dalam bidang automotif atau dalam bidang komponen-komponen industri. Enjin boleh dipanggil sebagai hati untuk sebuah kereta dan piston boleh juga di ketegorikan perkara yang amat penting dalam bahagian enjin. Terdapat ramai pengkaji yang mengkaji tentang piston enjin, geometri terbaru, bahan dan teknik pemprosesan dan pengkembangan ini telah berterusan berkembang hingga lebih terperinci. Walaupun pengkaji masih lagi mengkaji tentang piston enjin, kini masih banyak piston yang rosak. Mekanisme kerosakan mempunyai pelbagai titik permulaan dan kebanyakannya adalah haus, suhu dan kelesuan.

Projek ini hanya tertumpu kepada analisis kesan keatas kerosakan kelesuan dan mengkaji tahap ketahanan piston kesan daripada suhu dan tekanan di dalam pembakaran dalaman enjin. Piston ini diambil daripada enjin diesel dan diubah suai agar boleh digunakan di dalam CNG enjin. Tempat yang paling kerap berlakunya kerosakan seperti pada permukaan atas piston dan dinding piston. Satu ujikaji mengenai kelesuan haba dan kelesuan mekanikal kerosakan di kaji.

# LIST OF TABLES

# LIST OF FIGURES

.

## LIST OF ABBREVIATIONS

| | |
|---|---|
| CNG | Compressed natural gas |
| LPG | Liquid gas |
| RON | Relatively octane number |
| BDC | Bottom dead centre |
| TDC | Top dead centre |
| CAE | Computer-aided engineering |
| MEP | Mean effective pressure |
| CMM | Coordinate measuring machine |
| FEA | finite element analysis |

## LIST OF SYMBOLS

| | |
|---|---|
| *Vbowl* | Bowl volume |
| *Vbdc* | Bottom dead center volume |
| *Vswept* | Swept volume |
| *Vclearance* | Clearance volume |
| *Cr* | Compression ratio |
| *Db* | Bowl diameter |
| *Vs* | Swept volume |
| *Vc* | Clearance volume |
| *Vtdc* | Top dead center volume |
| *h* | Height of bowl |
| $\sigma_f$ | True tracture strength |
| $S_f$ | Fatigue strength |
| $S'_f$ | Fatigue strength coefficient |

# CHAPTER 1

# INTRODUCTION

## 1.1 Background

Global environment pollution gives effect to many health problems world wide. Therefore extensive studies have been conducted all over the world to use alternative fuels such as alcohol, ether and gaseous fuels (CNG & LPG) which can reduce the air pollution level by existing fuels (Petrol & Diesel) & bring a sigh of relief. CNG means Compressed Natural Gas. Its main constituents are Methane (90-95%) & marginal quantities of Propane, Iso-Butane & Butane. Natural Gas is stored in cylinders under high pressure of about 200 bars.

CNG is cheaper in price thus saves more on compared to petrol and diesel. Another advantage of having high octane number is drastic reduction in pollution thus making CNG less dangerous. In case of leakage it dissipates very easily in air as it is lighter than air & risk of any hazard is considerably reduced and CNG is available. CNG is available in abundant quantity in the earth's crust. It leads to higher thermal efficiency. It is non toxic.

In recent years, CNG has been promoted as a promising clean fuel alternative to spark ignition engines because of its relatively higher octane level. Due to its high research octane number (RON>130), CNG allows the combustion at higher compression ratio without knocking. It also offers much lower greenhouse gas emissions than those from the burning of other hydrocarbons as a result of its higher hydrogen to carbon ratio. Recently, the exact understanding of the physical and chemical processes is required to speed up the design process due to the increasing market demands of making new engines.

## 1.2 Problem Statement

- 2D analysis using 8 types of meshing density and for 3D analysis using 4 types meshing percentage.
- The compression ratio is range 12- 17.

## 1.3 Objective

- To design piston model 2D and 3D appropriate with real dimension.
- To analyze the design with finite element analysis (FEA)

## 1.4 Project Scope

- Modification of piston diesel engine.
- To understand the function of piston and its material properties.
- To convert the diesel engine into CNG engine.

### 1.4 Gantt Chart FYP 1

Table 1.1: Gantt Chart/ Project Schedule For FYP 1

| GANTT CHART/ PROJECT SCHEDULE FOR FYP 1 | | | | | | | | | | | | | | | | | |
|---|---|---|---|---|---|---|---|---|---|---|---|---|---|---|---|---|---|
| | PROJECT ACTIVITIES | WEEKS | | | | | | | | | | | | | | | |
| | | 1 | 2 | 3 | 4 | 5 | 6 | 7 | 8 | 9 | 10 | 11 | 12 | 13 | 14 | 15 | 16 |
| 1 | Discuss on the title of the FYP 1 | | | | | | | | | | | | | | | | |
| 2 | Discuss on the objectives and the scopes of the FYP 1 | | | | | | | | | | | | | | | | |
| 3 | Chapter 1 include the objectives, scopes, and the problem statements | | | | | | | | | | | | | | | | |
| 4 | Submit the chapter 1. Discuss on the format of project | | | | | | | | | | | | | | | | |
| 5 | Literature study. Find the information related to the literature review | | | | | | | | | | | | | | | | |
| 6 | Discuss on chapter 2, the literature review, journal and related information | | | | | | | | | | | | | | | | |
| 7 | Chapter 2.1, the introduction of piston. | | | | | | | | | | | | | | | | |
| 8 | Discuss on chapter 2.1 | | | | | | | | | | | | | | | | |
| 9 | Chapter 2.2, introduction of CAE and CAD and method analysis | | | | | | | | | | | | | | | | |
| 10 | Discuss on the analysis and the methodology | | | | | | | | | | | | | | | | |
| 11 | Chapter 3, The methodology | | | | | | | | | | | | | | | | |
| 12 | Preparation for the presentation | | | | | | | | | | | | | | | | |

### 1.5 Gantt Chart FYP 2

Table 1.2: Gantt Chart/ Project Schedule For FYP 2

| GANTT CHART/ PROJECT SCHEDULE FOR FYP 2 | | | | | | | | | | | | | | | | | |
|---|---|---|---|---|---|---|---|---|---|---|---|---|---|---|---|---|---|
| | PROJECT ACTIVITIES | WEEKS | | | | | | | | | | | | | | | |
| | | 1 | 2 | 3 | 4 | 5 | 6 | 7 | 8 | 9 | 10 | 11 | 12 | 13 | 14 | 15 | 16 |
| 1 | Forms filled to use the laboratory lab (CMM room) | | | | | | | | | | | | | | | | |
| 2 | Literature Review | | | | | | | | | | | | | | | | |
| 3 | Measure the dimension of piston | | | | | | | | | | | | | | | | |
| 4 | Design 2D analysis using Algor software | | | | | | | | | | | | | | | | |
| 5 | Design Piston 3D using solidwork software | | | | | | | | | | | | | | | | |
| 6 | Discussion on analysis, the constraint, load | | | | | | | | | | | | | | | | |
| 7 | Analysis the assembly using the Algor software | | | | | | | | | | | | | | | | |
| 8 | Conclusion based on discussion | | | | | | | | | | | | | | | | |
| 9 | Discussion on chapter 4 and 5 | | | | | | | | | | | | | | | | |
| 10 | Discuss on the analysis and the methodology | | | | | | | | | | | | | | | | |
| 11 | Preparations for presentation 2 | | | | | | | | | | | | | | | | |
| 12 | Final report submission | | | | | | | | | | | | | | | | |

# CHAPTER 2

# LITERATURE REVIEW

## 2.1 COMPRESSED NATURAL GAS (CNG)

### 2.1.1 Typical composition of natural gas

2.18% nitrogen, 92.69% methane, 3.43% ethane, 0.52% carbon dioxide, 0.71% propane, 0.12% *iso*-butane, 0.15% *n*-butane, 0.09% pentane and 0.11% hexane.

Table 2.1: Parameter of compressed natural gas fuel [19].

| **Parameter** | **CNG Fuel** |
|---|---|
| Relative Density of diesel fuel | 0.844 |
| Viscosity | 0.045 |
| Net Calorific Value | 34.83 MJ/$m^3$ |
| Gross calorific value | 38.59 MJ/$m^3$ |
| Net calorific value of diesel fuel | 42.70 MJ/kg |
| Gross Wobbe number | 49.80 MJ/$m^3$ |
| Stoichiometric air/fuel ratio | 14.5:1 |

Source: John B. Heywood. McGRAW-HILL (2009)

### 2.1.2 Rated power (using CNG fuel)

CNG has higher values for these ratios, which means that CNG has higher potential to convert initial fuel availability to do useful work, even without taking advantage of its higher octane number rating. If compression ratio is raised, it can be expected that CNG fuelling would outperform the gasoline fuelled engine in both the IMEP and the second law efficiencies [7]. CNG has higher availability transfer with work (38.2%) than gasoline operation (33.4%). Availability destruction due to

combustion is about the same for CNG and gasoline. However, availability destruction due to heat transfer is lower with CNG operation (13.8%).

## 2.2 EXPERIMENTAL REVIEW

### 2.2.1 Setup and Procedures

Referring to research conducted by Ke Zheng etall [6], A single cylinder engine was modified into a natural gas direct-injection engine. To increase the flow rate for natural gas application, the swirler near the tip of nozzle was taken off. Natural gas is injected into cylinder at the constant pressure of 8 MPa. Besides installing the natural gas high-pressure injector, a spark plug is also installed into the centre of combustion chamber as the ignition source.

Table 2.2: Engine specifications [6]

| **Engine specifications** | |
|---|---|
| Bore (mm) | 100 |
| Stroke (mm) | 115 |
| Displacement (cm3) | 903 |
| Compression ratio | 8 |
| Injection pressure (MPa) | 8 |
| Ignition source | Spark plug |
| Combustion chamber | Bowl-in-shape |

Source: Ke Zeng, Zuohua Huang (2006)

## 2.3 INTERNAL COMBUSTION ENGINE

The compressed ignition or diesel engine had been developed by Rudolf Diesel in 1892 [1]. The normal internal combustion engine is generally one of two types, spark ignition petrol or gas engines and diesel engine [2]. In this engine, the piston reciprocates in the cylinder between two fixed position called the top dead centre (TDC) and the bottom dead centre (BDC) [3][4]. TDC is the position of the piston when it forms the smallest volume in cylinder and BDC is the position of the piston when it forms the largest volume in the cylinder. The distance between TDC

and BDC is called the stroke of the engine while the diameter of the piston is called the bore [3]. The minimum volume formed in the cylinder when the piston is at TDC is called the clearance volume while the displacement volume is the volume displaced by the piston as it moves between TDC and BDC [3]. The compression ratio is the ratio of maximum volume formed in the cylinder to the minimum volume [3][5].

$$r = \frac{Vmax}{Vmin}$$

Equation 2.1.1: Compression ratio [3]

The other important term that is frequently being used in conjunction with reciprocating engine are the mean effective pressure (MEP). It is a fictitious pressure that, if it acted on the piston during the entire power stroke, would produce the same amount of net work as that produced during the actual cycle [3].

$$MEP = \frac{Wnet}{Vmax - Vmin}$$

Equation 2.1.2: Mean effective pressure [3]

## 2.4 PISTON

### 2.4.1 Introduction

The piston is one of the most stressed components of an entire vehicle. Pressures at the combustion chamber may reach about 180–200 bar [10]. Speeds reach about 25 m/s and temperatures at the piston crown may reach about 400 °C [10]. As one of the major moving parts in the power-transmitting assembly, the piston must be designed so that it can withstand the extreme heat and pressure of combustion. Pistons must also be light enough to keep inertial loads on related parts to a minimum. It also transmits heat to the cooling oil and some of the heat through the piston rings to the cylinder wall [14].

Notwithstanding this technological evolution there are still a significant number of damaged pistons. Damages may have different origins: mechanical stresses, thermal stresses, wear mechanisms, temperature degradation, oxidation mechanisms and etc. Fatigue is a source of piston damages. Although, traditionally, piston damages are attributed to wear and lubrication sources, fatigue is responsible for a significant number of piston damages. And some damages where the main cause is attributed to wear and/or lubrication mechanisms may have in the root cause origin a fatigue crack.

Fatigue exists when cyclic stresses/deformations occur in an area on a component. The cyclic stresses/deformations have mainly two origins: load and temperature. Traditional mechanical fatigue may be the main damaging mechanism in different parts of a piston depending on different factors. High temperature fatigue (which includes creep) is also present in some damaged pistons. Thermal fatigue and thermal–mechanical fatigue are also present in other damaged pistons. A finite element linear static analysis, using “cosmos works”, is used for stress and temperature determination. Only aluminum pistons are assessed in this work because most of the engine pistons are in aluminum.

The fatigue-damaged pistons may be divided into two categories: the mechanical and high temperature mechanical damaged pistons and the thermal and thermal–mechanical damaged pistons. The mechanical and high temperature mechanical damaged pistons may be divided according to the damaged area: piston head; piston pin holes; piston compression ring grooves; and piston skirt. The analysis, in this work, will be made according to this classification.

### 2.4.2 Mechanical and high temperature mechanical fatigue

By mechanical fatigue means that in a piston a crack will nucleate and propagate in critical stressed areas. The stresses in this context are due to the loads acting externally on the piston. Although stresses on pistons change with piston geometries and engine pressures, Figure 2.1 and Figure 2.2 show a typical stress distribution on an engine piston. In Figure 2.1 and Figure 2.2 pressures are merely indicative and are used only with the purpose of determination of the most stressed

areas. It is not intended to determine the real stresses acting on the piston. The dynamic and thermal stresses are not also included in Figure 2.1 and Figure 2.2.

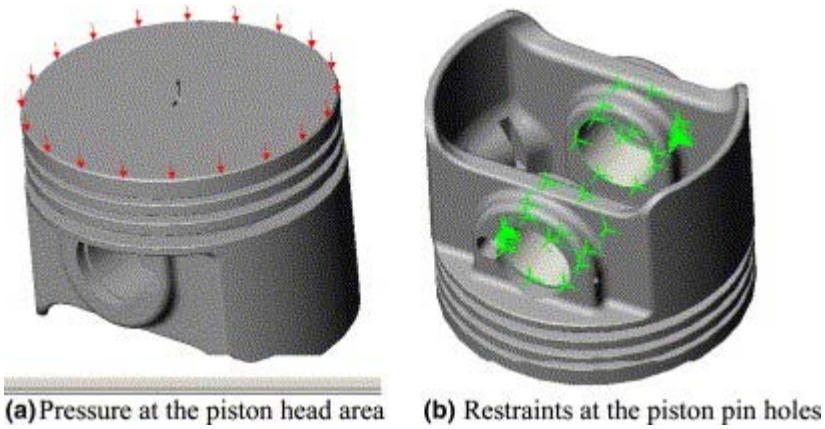


Figure 2.1: Typical engine piston [14]

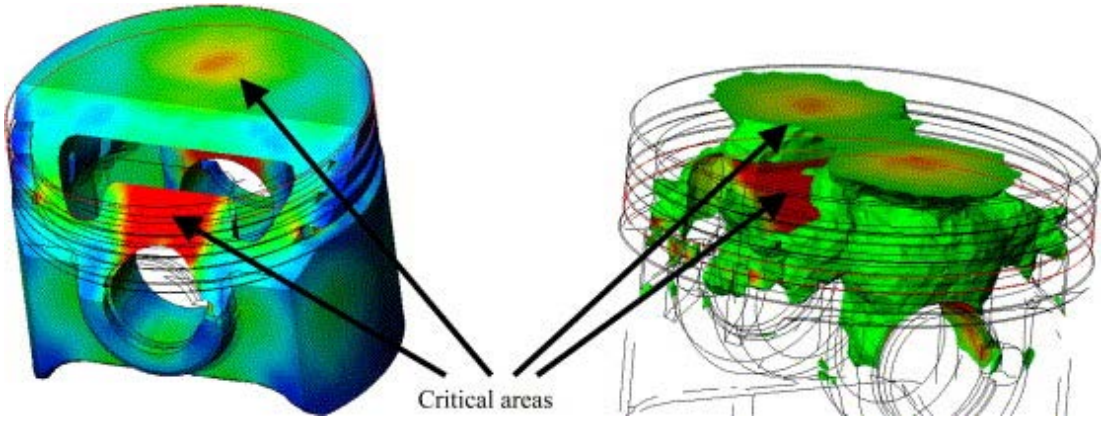


Figure 2.2: Typical stress distribution on an engine piston [14].

It is clear that there are mainly two critical areas: the top side of piston pin hole and two areas at the piston head. Stress analyses on diesel pistons show the same critical areas. If holes or grooves are introduced on the pin hole it is possible to introduce critical stressed areas on those discontinuities.

### 2.4.3 Piston head and piston pin hole

As observed in Figure 2.1 and Figure 2.2, due to the pressure at the piston head, there are mainly two critical areas: piston pin holes and localized areas at the piston head. On pistons in Figure 2.3 and Figure 2.4 the cracks initiated on the piston head near the combustion chamber.

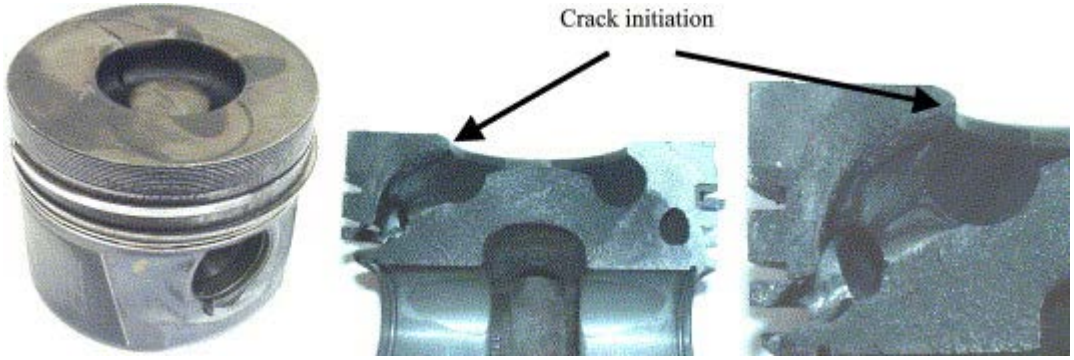


Figure 2.3: Diesel engine piston (with cooling gallery) with a crack from one side of the pin hole to the head [14]


Figure 2.4: Diesel engine piston with a crack from one side of the pin hole to the other pin hole going through the head of the piston [14].

A FEM analysis, Figure 2.5 was made to piston of Figure 2.4 and the results show that in pistons with a bowl combustion chamber, besides the pin holes (and in this particular case on the curvature radius on the inner side of the piston top) there are also two regions at the piston head where there exist stress concentrations. These two areas are located on the same vertical plane that contains the pin holes.

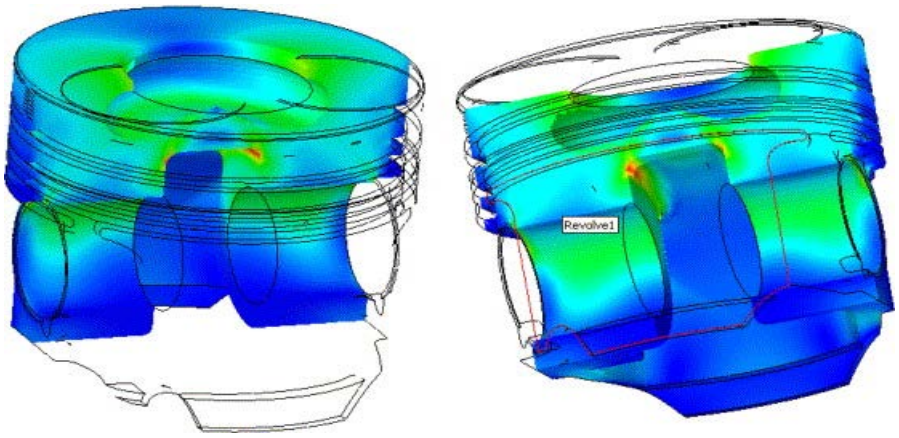


Figure 2.5: Linear static stress distribution of piston in Figure 2.4 [14].

### 2.4.5 Piston Skirt

Another common fatigue damage that occurs in pistons is related to broken skirts, as shown in Figure 2.6.

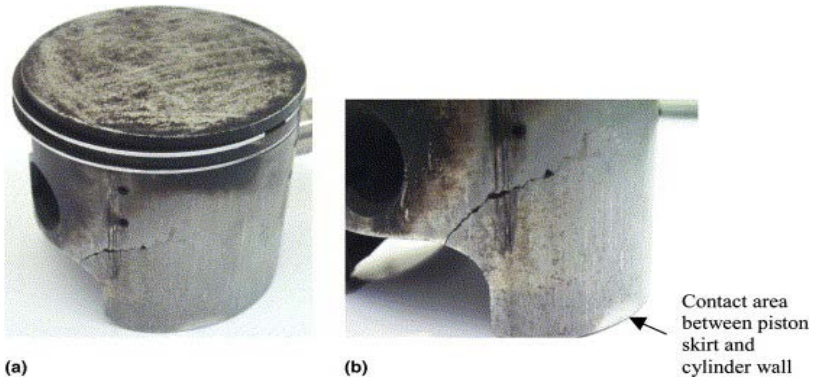


Figure 2.6: Engine piston with damaged skirt: (a) piston; (b) detail of damaged skirt [14].

In Figure 2.6 is clear the crack (on the other side there is another crack) emanating from the curvature radius on the skirt. In Figure 2.9 a simulation is made for stress analysis in piston skirt for a specific angle in respect to the vertical axis.

### 2.4.6 Thermal/thermal–mechanical fatigue

Thermal stresses are difficult to simulate because there are, in a piston, two kinds of thermal stresses (see Figure 2.7):

(a) Thermal stresses due to the ‘vertical’ distribution of the temperature along the piston – high temperatures at the top and lower temperatures at the bottom.

(b) Thermal stresses due to the different temperatures at the head of the piston due to the flow of the hot gases or to fuel impingement (related to high-pressure injection).

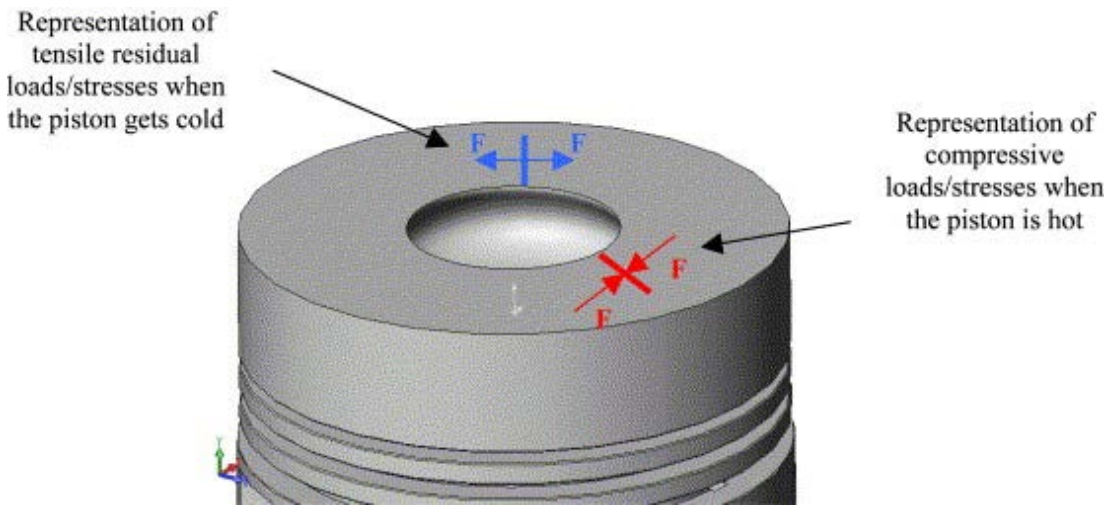


Figure 2.7: Sketch of an example of thermal stresses at the top of a piston and forces, F, acting on the material [14].

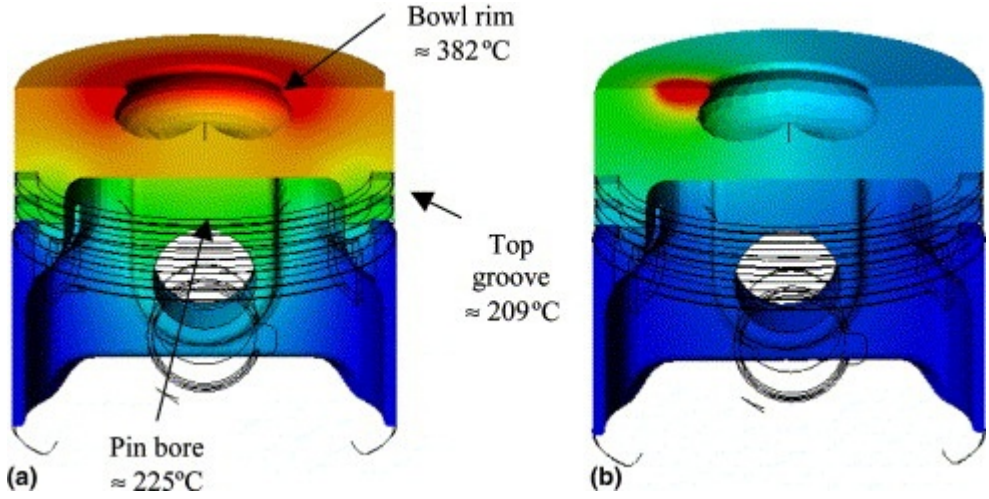


Figure 2.8: Schematic thermal distribution at a piston: (a) homogeneous; (b) localized.

(b) Thermal stresses due to the different temperatures at the head of the piston are represented in Figure 2.8(b). This distribution causes localized warmer areas. The mechanism under which the thermal cracks form is the same as mentioned in Figure 2.8(a) with the exception that in this case these warmer areas will have higher compressive stresses – followed by creep – followed by higher tensile stresses when the piston gets cold. Thus, in this case is most probable that localized areas at the bowl rim will concentrate the thermal fatigue cracks.

In the first case, Figure 2.8(a) it would be expected several fatigue radial cracks over the whole piston head. In the second case, Figure 2.8(b) it would be expected fatigue cracks in specific areas of the piston head (those where the thermal gradients occur). Together with the mechanical load due to peak cylinder pressure, the bowl rim experiences cyclic load in the compressive range. After creep relaxation of the high compressive stresses, alternating fatigue loading, at least along the pin axis, may occur.

### 2.4.7 Mechanical fatigue

Mechanical fatigue damages at piston head and piston pin holes is the reason of several damaged engine pistons. Static stresses concentrate mainly at pin holes. This explains cracks initiated at piston pin holes. The reason for the crack to initiate at that point at the piston rim area may be related to two different aspects:

• Mechanical fatigue: The cracks always initiate at the same points .The stresses at the piston head are higher at those areas. However, the reason why the crack initiated at the head instead of the pin hole, where the stresses are higher, is not answered yet. The reason may be on temperature.

• High temperature mechanical fatigue: There is a temperature distribution along the vertical axis of the piston. The head is always hotter than the bottom and the pin hole area. Thus the fatigue resistance of the material at the head is lower even though the material is the same [16]. In diesel engine pistons the areas where the temperature is higher is right at the bowl rim of the piston, where the temperature may reach about 382 °C. Thus, the edge area at the combustion chamber bowl rim is the less resistant due to the high temperature. Thus, depending on the particular geometry of each piston, and taking into account both the static stresses and the temperature influence on the material resistance, either the pin hole area and the bowl rim area may be critical. For a comparison, temperatures on the pin hole may reach about 225 °C at the same piston where temperature at the bowl rim area reaches about 382 °C. At the same time temperature at the top groove is about 209 °C.

### 2.4.8 Materials

For many years the eutectic Al–Si alloy has been used for pistons (because only aluminum pistons have been assessed in this work only aluminium alloys will be presented). With increased piston temperatures, the need for equal or improved fatigue strength could no longer be satisfied. New alloys with increased Si content and Cu content, and other alloying elements, have been proved be satisfactory to the new requirements [17][18]. Use of metal matrix composites is already in use and also under investigation [4][5][6]. For the future, additional improvements of the materials properties may be expected. Other technologies and die-casting processes are also being developed [16][17].

# CHAPTER 3

# METHODOLOGY

## 3.1 INTRODUCTION

This chapter represents the method and process occurred while carrying out this project. All of the processes like measuring the parameter, and simulating the model will be explained clearly in this chapter. Also, the tools and software used for this project will also be described.

From initial stage

Learning on how to use calpso software with it machine. Calpso software and its machine are part of coordinate measuring machine (CMM). Calpso software is the software that helps students to get the accurate dimension without using vernier calliper. Do some reverse engineering on the piston to get its dimension with Calpso software. From that dimension, generate 3D drawing using Solidwork software.

Second stage

By using Solidworks, design the 3D piston appropriates to the original piston dimension. Simulation on heat transfer and stress of the design to ensure that the design will not fail in real case. This can be performed by using finite element analysis (FEA) by Algor software.

## 3.2 MEASURING THE PARAMETER OF THE ENGINE

The parameter of the piston can be measured in two ways. Firstly, the conventional method where a vernier caliper is used to measure the real piston engine's parameter. All of the parameters required simulating the piston in 3-D modeling such as; bore, stroke, diameter of the piston, height of the bowl etc. will be measured precisely using the vernier caliper to get more accurate value.

Secondly, using the Solidworks drawing as shown in Figure 3.1 where all the parameters can be obtained directly from the 3-D drawing. The function of this way is to compare the value obtained from the conventional method and the Solidworks drawing. For quick and accurate measuring, the Solidworks drawing also can be used.

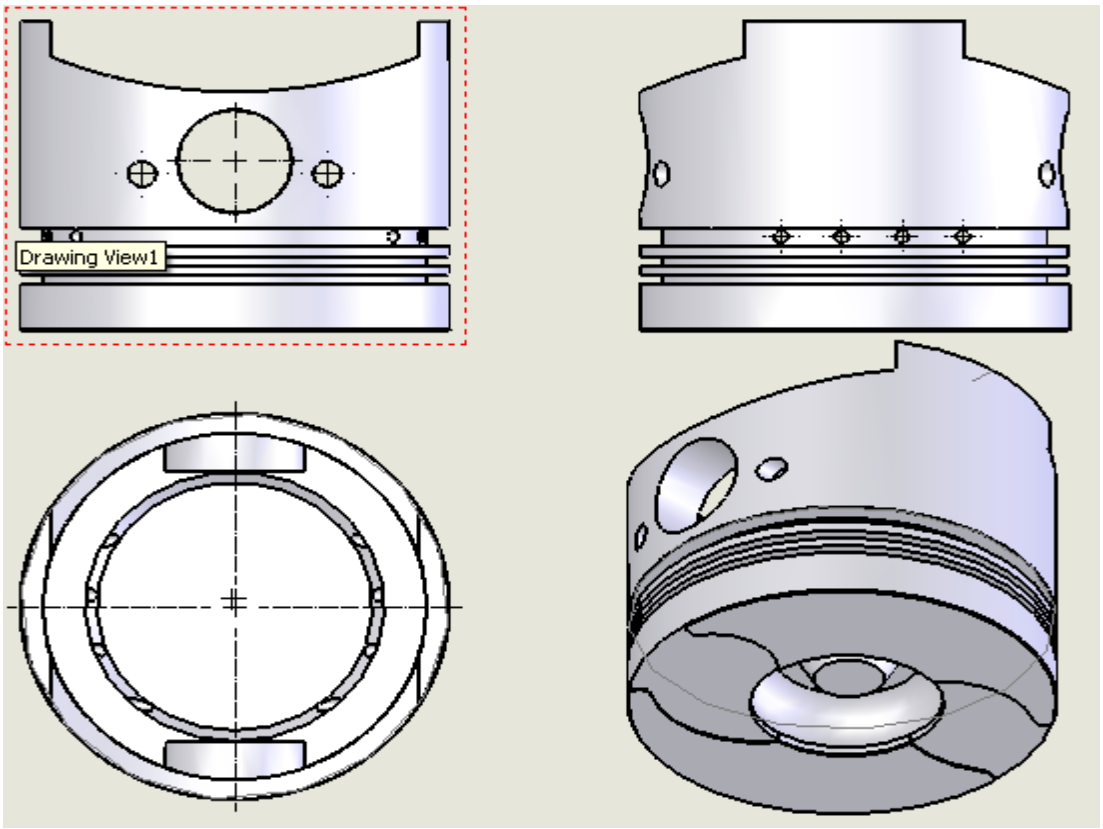


Figure 3.1: Solidworks drawing for piston engine

### 3.3 2D ANALYSES

#### 3.3.1 Parameter of Piston in the internal combustion engine diesel

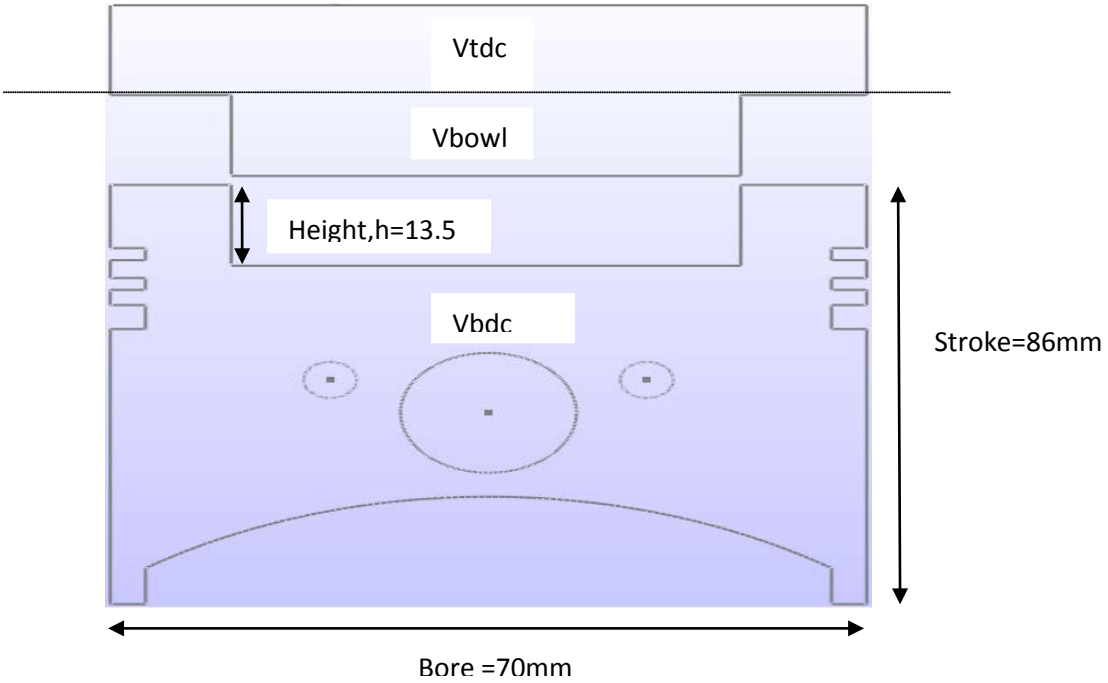


$Vbowl = 17.6 \times 10^3\ mm^3$

$Vbdc = \pi/4 \times (B^2)(S)$

$= \pi \div 4 \times (86^2)(70)$

$= 406616.34\ mm^3$

$Vswept$ = Vbowl + Vbdc

$= 17.6 \times 10^3 + 406616.34$

$= 424216.34\ mm^3$

$Vclearance = Vtdc + Vbowl$

$Vclearance = \frac{\pi}{4}(d^2)(TDCclearance) + Vbowl$

$= \frac{\pi}{4}(86^2)(0.6) + 17.6 \times 10^3$

$= 21085.28 mm^3$

Compression Ratio, $Cr = \frac{Vs + Vc}{Vc}$

$$= \frac{424216.34 + 21085.28}{21085.28}$$

$= 21.12$

### 3.3.2 Parameter of Piston in the internal combustion CNG engine

From the literatture review, compression ratio is 14.5 shown high performance and ideal. When compression ratio changes, the value for Volume Bowl (Vbowl) also change.

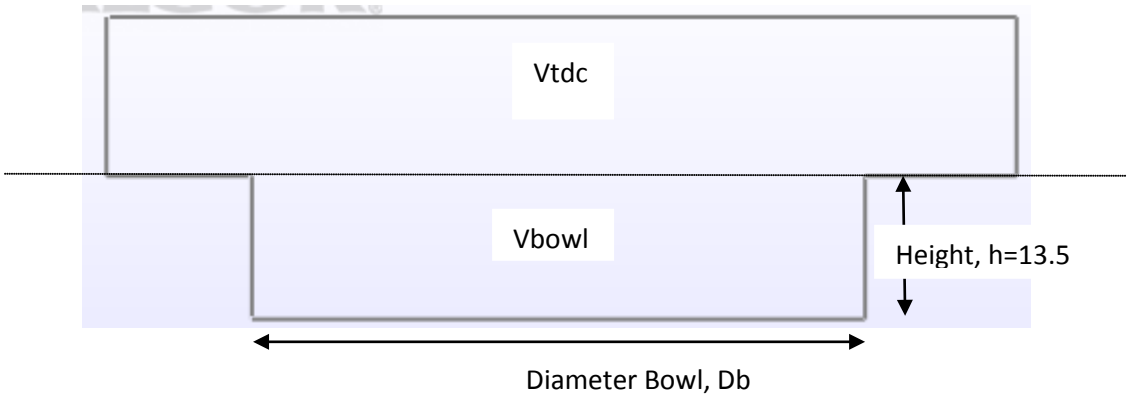


$Vbowl = \frac{\pi}{4} \times (Db^2)(h)$

$= \frac{\pi}{4} \times (Db^2)(13.5)$

? = $Db^2$

$Cr = \frac{Vs+Vc}{Vc}$

$= \frac{(Vbdc+Vbowl)+Vc}{Vc}$

$$14.5 = \frac{\left(406616.34+\frac{\pi}{4}\times(\boldsymbol{Db^2})(\mathbf{13.5})\right)+\frac{\pi}{4}(d^2)(TDCclearance)+Vbowl}{\frac{\pi}{4}(d^2)(TDCclearance)+Vbowl}$$

$$14.5 = \frac{\left(406616.34+\frac{\pi}{4}\times(\boldsymbol{Db^2})(\mathbf{13.5})\right)+\frac{\pi}{4}(86^2)(0.6)+\frac{\pi}{4}\times(Db^2)(13.5)}{\frac{\pi}{4}(86^2)(0.6)+\frac{\pi}{4}\times(Db^2)(13.5)}$$

$50536.6 + 153.74Db^2 = 406616.34 + 10.603Db^2 + 3485.28 + 10.60Db^2$

$153.74Db^2 + 359565.02 = 21.2Db^2$

$132.54Db^2 = 359565.02$

$Db^2 = 2712.88$

$Db = 52.08$mm

Creating Formula in Microsoft Excell

$$Cr = \frac{Vs+Vc}{Vc}$$

$$Cr = \frac{(Vbdc+Vbowl)+(Vtdc+Vbowl)}{(Vtdc+Vbowl)}$$

$$\mathrm{Cr}(Vtdc + Vbowl) = (Vbdc + Vbowl) + (Vtdc + Vbowl)$$

$$\mathrm{Cr}(Vtdc) + Cr(Vbowl) = (Vbdc) + Vtdc + 2Vbowl)$$

$$Cr - 2(Vbowl) = (Vbdc) + Vtdc - CRVtdc$$

$$(Vbowl) = \frac{(Vbdc + Vtdc - CRVtdc)}{CR-2}$$

$$Db = \sqrt{\frac{4(Vbdc + Vtdc - CRVtdc)}{\Pi h(CR-2)}}$$

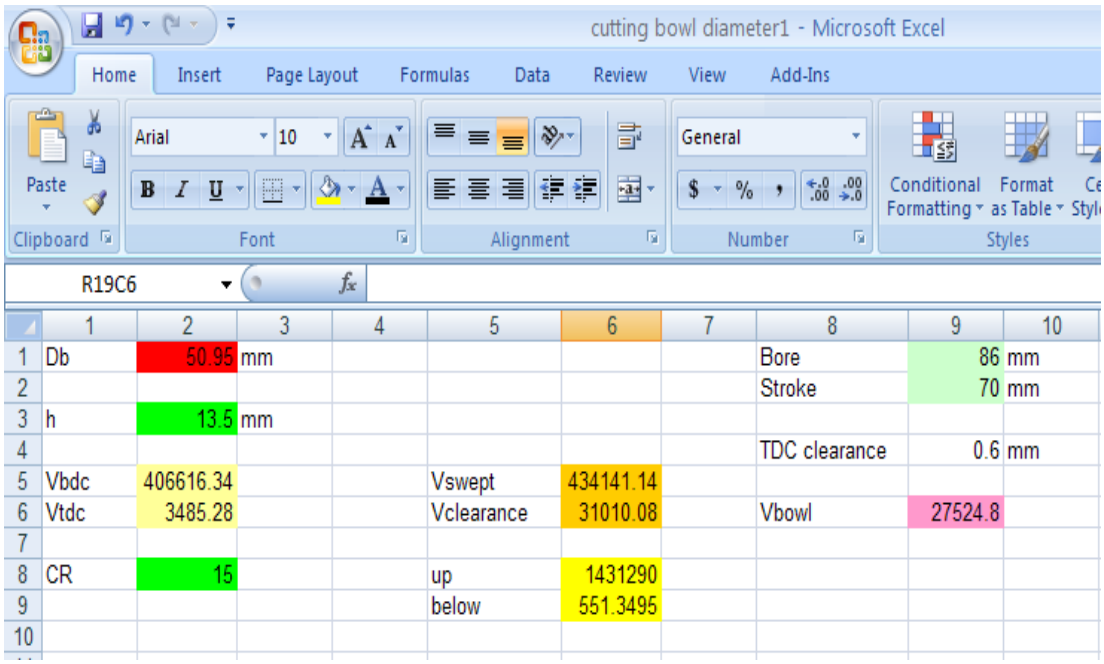


| | 1 | 2 | 3 | 4 | 5 | 6 | 7 | 8 | 9 | 10 |
|---|---|---|---|---|---|---|---|---|---|---|
| 1 | Db | 50.95 | mm | | | | | Bore | 86 | mm |
| 2 | | | | | | | | Stroke | 70 | mm |
| 3 | h | 13.5 | mm | | | | | | | |
| 4 | | | | | | | | TDC clearance | 0.6 | mm |
| 5 | Vbdc | 406616.34 | | | Vswept | 434141.14 | | | | |
| 6 | Vtdc | 3485.28 | | | Vclearance | 31010.08 | | Vbowl | 27524.8 | |
| 7 | | | | | | | | | | |
| 8 | CR | 15 | | | up | 1431290 | | | | |
| 9 | | | | | below | 551.3495 | | | | |
| 10 | | | | | | | | | | |

Figure 3.2: Formula generated on Microsoft Excel.

### 3.3.3 Geometry of 2D Design

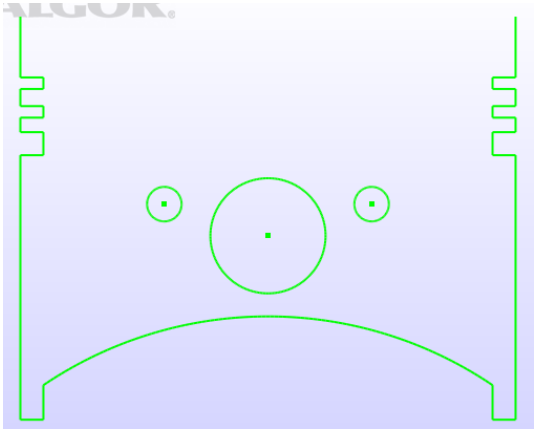

Figure 3.3: Sketching 2D model

Firstly, open the Algor Fempro Software. After that, click on  new model wizard. New box will appear and select  and  and then press open. On the design scenario, click for single analysis statics stress with linear material models and press button ok. In Unit definition, change the length in meter (m) to millimeter (mm) by change the unit system in custom. Remember that unit system is metric mks (SI) before change the length unit.

Second step is press button new sketch  and click ok on select plane to proceed. Start input value and follow step bellow.

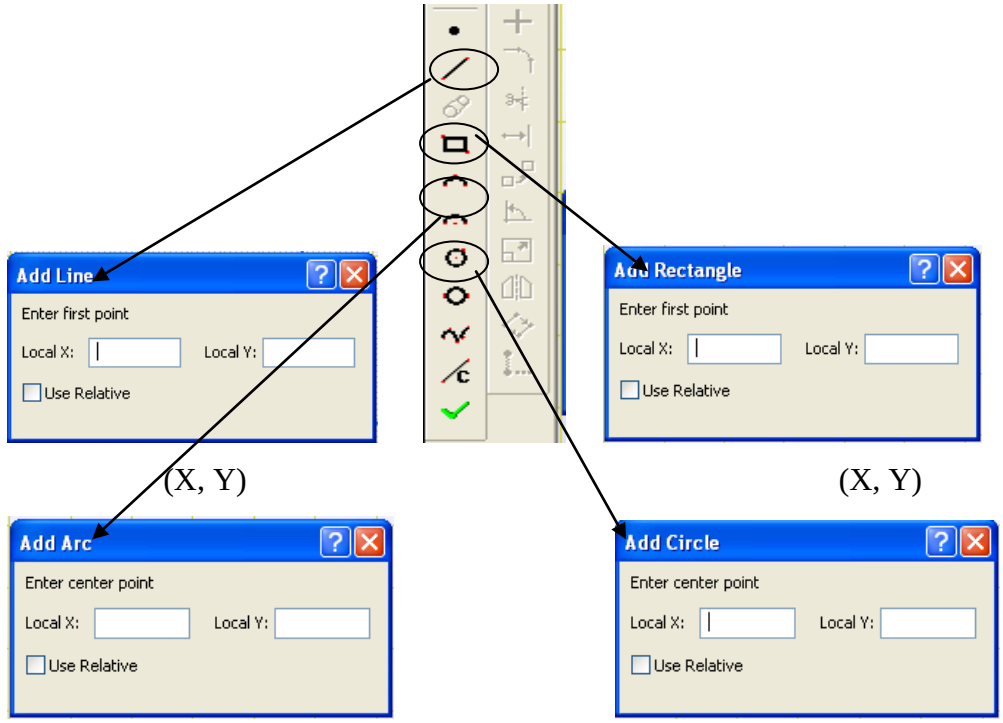


Add rectangular and put value (0, 0), (86, 70)

Add Line and put value (0, 70), (0, 59.44), (4, 59.44)
(4, 57.44), (0, 57.44)
(0, 54.46), (4, 54.46)
(4, 52.46), (0, 52.46)
(0, 49.94), (4, 49.94)
(4, 45.94), (0, 45.94), (0, 0)

Add Line and put value (86, 70), (86, 59.44), (82, 59.44)
(82, 57.44), (86, 57.44)
(86, 54.46), (82, 54.46)
(82, 52.46), (86, 52.46)
(86, 49.94), (82, 49.94)
(82, 45.94), (86, 45.94), (86, 0)

Add line and put value (0, 0), (4, 0), (4, 6)

Add line and put value (86, 0), (82, 0), (82, 6)

Add circle and put value (43, 41.94), (43, 21.94)

Add three point arc and put value (4, 6), (82, 6), (43, 17,94)

Add circle and put value (28, 37.44), (22, 37.44)

Add circle and put value (58, 37.44), (64, 37.44)

| Compression Ratio | 1 | 2 | Diameter Bore,Db |
|---|---|---|---|
| 12.0 | 13.53 | 72.47 | 58.94 |
| 12.5 | 14.31 | 72.25 | 57.94 |
| 13.0 | 15.035 | 70.965 | 55.93 |
| 13.5 | 15.715 | 70.285 | 54.57 |
| 14.0 | 16.355 | 69.645 | 53.29 |
| 14.5 | 16.955 | 69.045 | 52.09 |
| 15.0 | 17.525 | 68.475 | 50.95 |
| 15.5 | 18.06 | 67.94 | 49.88 |
| 16.0 | 18.57 | 67.43 | 48.86 |
| 16.5 | 19.055 | 66.945 | 47.89 |
| 17.0 | 19.515 | 66.485 | 46.97 |

For example: compression ratio 12.0

Add line and put value (0, 70), (13.53, 70), (13.53, 56.5), (72.47, 56.5), (72.47, 70), (86, 70)

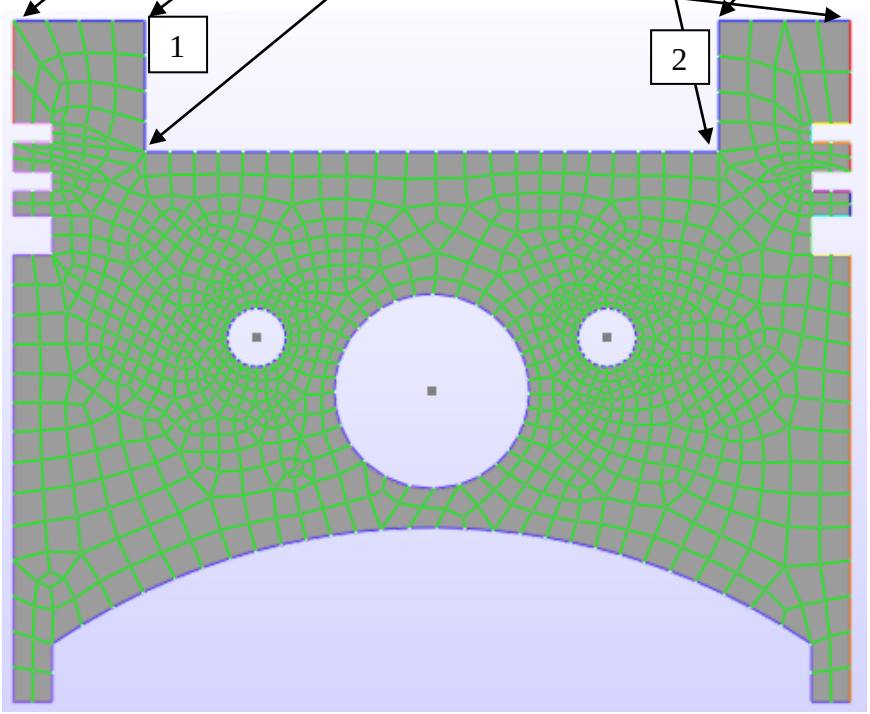

After that, press button generate 2-D sketch mesh  to display the corresponding panel. 2-D mesh generation will display and change value of mesh density to 500. Change value of mesh density is 500, 1000, 1500, 2000, 2500, 3000, 3500 and 4000. After completing 2D design model, it time to add pressure that applied on the piston head and fixed boundary condition at piston boss. The pressure is 70bar is equal to 7MPa.

70bar = 70 x 101.325kPa

= 7092.75kPa

= 7092750Pa

= 7MPa

7MPa = 7 $N/mm^2$

7 $MN/m^2$ = 7 $N/10^{-3}m^2$

7 $MN/m^2$ = 7 x $MN/m^2$

= Proved

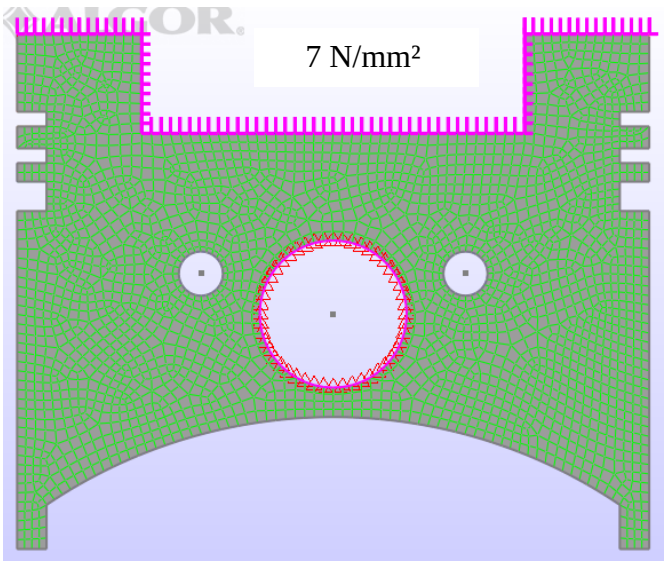


Select point select and select surfaces as shown as in the picture.  Right click and add surface load for 2-D element and put pressure 7 $N/mm^2$. Secondly, select plane pin boss and right click. Add surface boundary condition and click fixed at predefined.

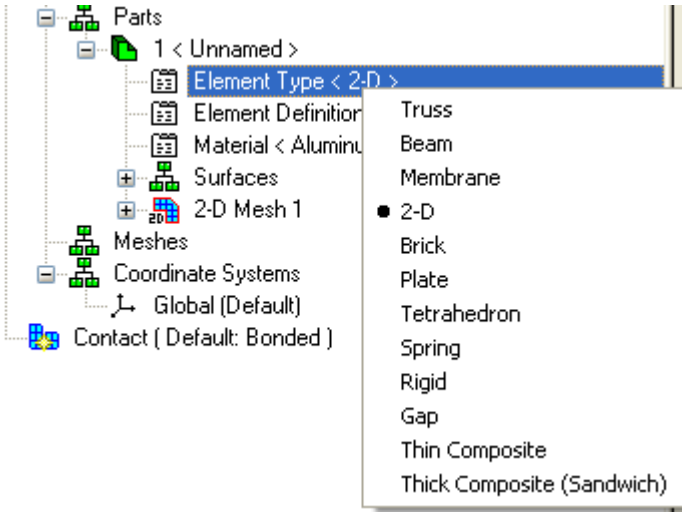


Choose 2-D for element type as shown above. After that, right click on element definition and modify element definition. The thickness is about 1mm and stress free reference temperature is 24ºC.

For the material, choose Aluminum 6061-T6;6061-T651(alloy). There are 2 material that includes in this analysis are Aluminum 6061-T6;6061-T651 and Cast iron.

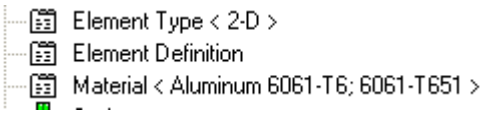


. Lastly run the analysis by pressing button perform analysis  and take data for Von mises stress, maximum principal stress, stress tensor Y-Y, displacement magnitude and von mises strain.

## 3.4 3D ANALYSES

Firstly design 3D model of piston in Solidwork software. After that, edit the diameter of bowl at the top piston corresponding to the compression ratio by Refering to the table 3.3.

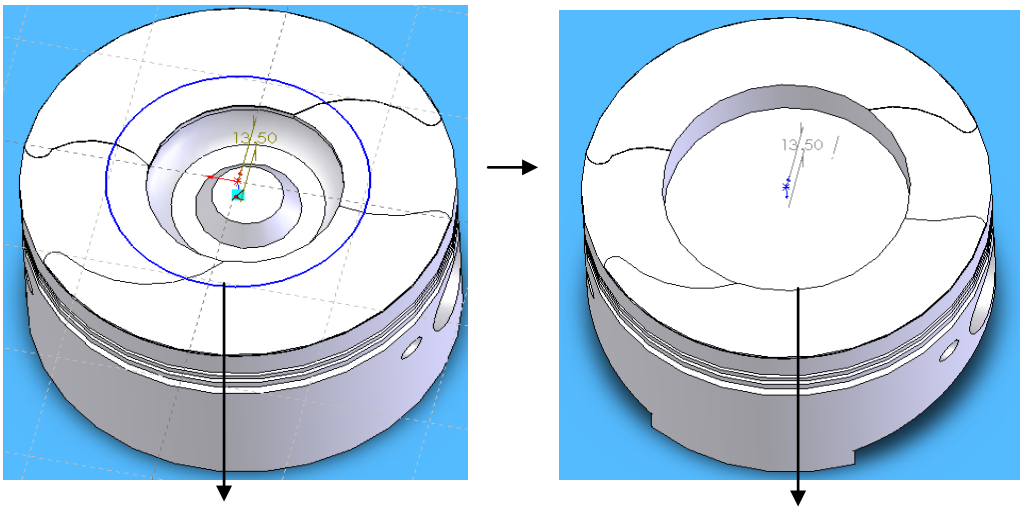


Diameter of bowl (sketch) at compression ratio 14.5

Diameter of bowl (after extrude)at compression ratio 14.5

Normally files in Solidwork is saved in type part, this time the file will be saved in type IGES to make it available to open in Algor software. Open the Algor software, click on button open file and open the files that have been saved.

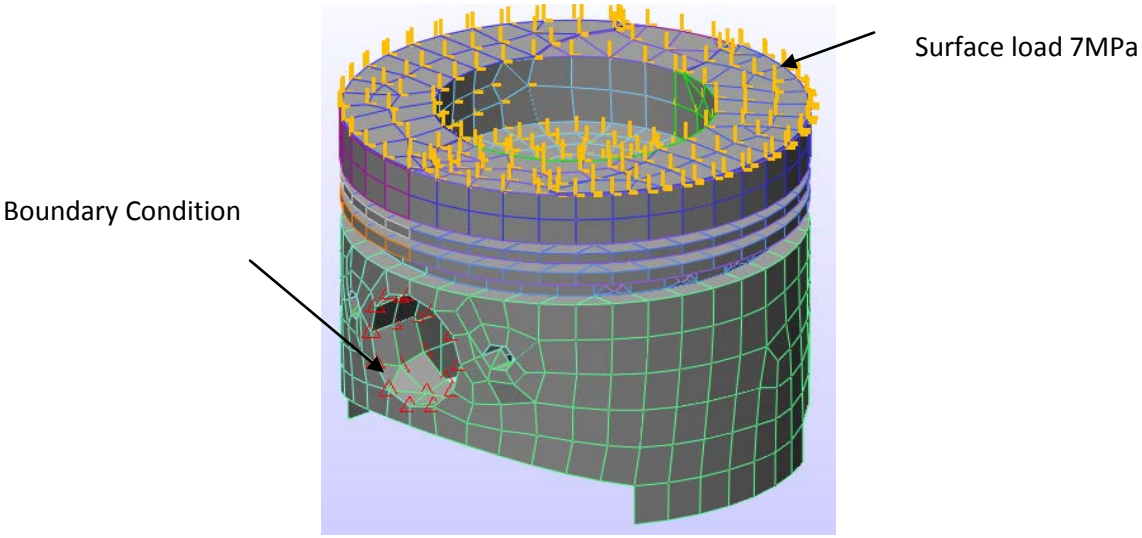


Another parameter and instruction just follow the way 2D to analysis.

## 3.5 PREPARING FINAL REPORT

After all the result is interpreted, the results will be arranged and displayed in the simplest form to make sure the results is understood. It is important to ensure the reader can understand all the results in only one reading. So, time is not wasted for the reader and they can go through the discussion section to know detail about the results. All of the results and discussions will finally be combined with the introduction, literature review and methodology to get the full final report.

## 3.6 FLOWCHART OF THE PROJECT

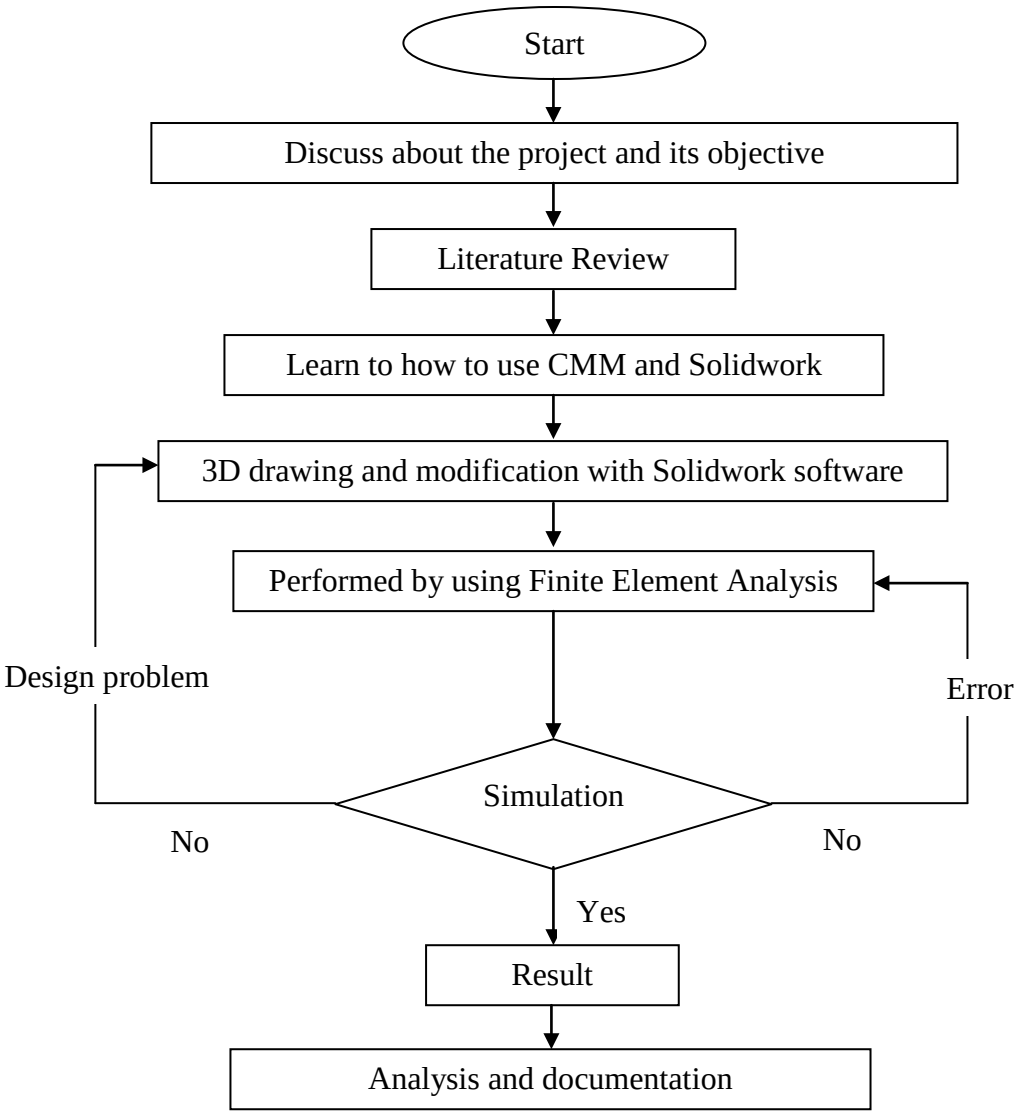

Flow Chart Description:

In the above flow chart, it started with discussion with co-supervisor about the project title, the objective of the project and what should do to complete the given task. After that, searching the information about piston on article and do some research and journal that related to the title. To continue the project, learn how to use calypso software and its machine operation. Next are the processes of reviewing and extracting the important facts, methods and results from all the articles. If the co-supervisor not satisfied with the proposal, repeat it again and if it is approved by the co-supervisor, so go to the next phase.

The project will be started by measuring the parameter of the dimension of fuel injector and its place on engine block. All of the parameter that will be used to created 2D and 3D model of piston. After finish designing the piston, all of the parameter that was recorded before it will be analyzes. For this step, I will be checking in and correct all the error. If it is satisfied with previous research, the data will be recorded as the final report.

# CHAPTER 4

# RESULTS AND DISCUSSION

## 4.1 INTRODUCTION

In this chapter, all of the raw results will be rearranged and the selected findings will be discussed briefly to give the proper explanation about the process and the important point in the results.

Table 4.1: Material Properties

| **Material** | **Aluminum(alloy) 6061-T6** |
|---|---|
| Density (kg/m³) | 2800 |
| Ultimate Strength Tension,(MPa) | 470 |
| Yield Strength, (MPa) | 410 |
| Modulus Of Elasticity, E (GPa) | 72 |
| Poisson's Ratio | 0.33 |
| Coefficient Of Thermal Expansion, 10¯6/°C | 23 |
| Thermal Conductivity (W/m º C) | 210 |

## 4.2 PRESSURE-3D ANALYSIS

### 4.2.1 Figure 3D Analysis

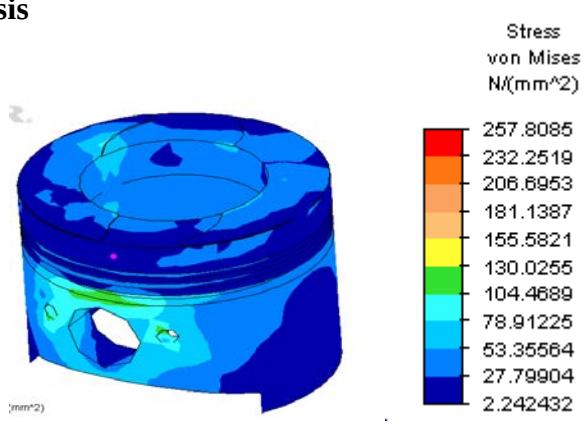


Figure 4.1: Maximum Von Mises Stress at Compression Ratio 14.5, 85%

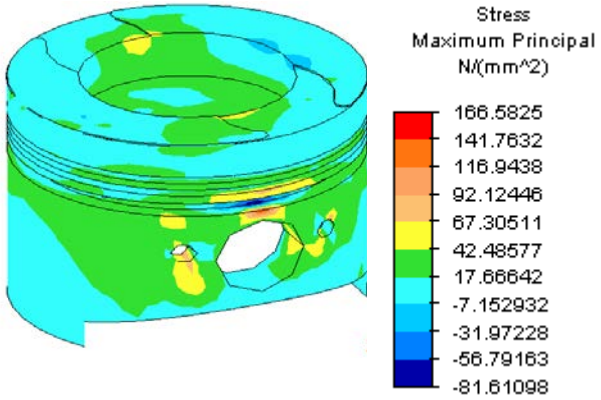


Figure 4.2: Maximum Principal Stress at Compression Ratio 14.5, 85%

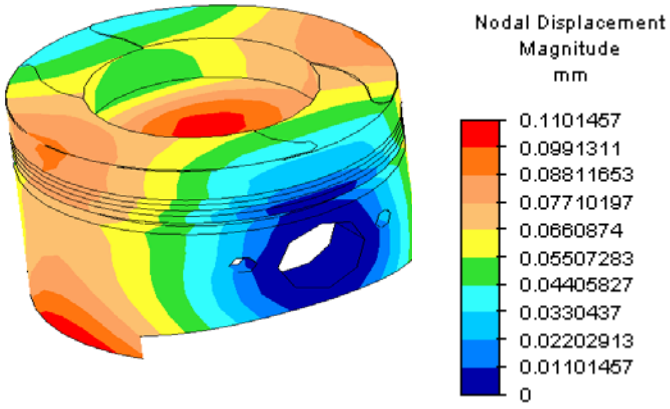


Figure 4.3: Nodal Displacement Magnitude at Compression Ratio 14.5, 85%

Figure 4.1, 4.2 and 4.3 are results for 3D analysis at compression ratio 14.5 and its percentage meshing is 85%. The maximum value for Von Mises Stress is about 257.8085 N/mm² or 257.8085MPa. The value is below than yield strength of the material and the material is undergoing elastic region. The maximum value for Maximum Principal Stress is 166.5825MPa and this value is below the Von Mises Stress value. The Von Mises Stresses is greater than a Maximum Principal Stress when one or both of the other stresses is negative (compressive). The maximum magnitude for Nodal Displacement is about 0.1101457mm. The value is acceptable for real piston to operate in internal combustion engine. Maximum stress concentration is located mostly at the edges of components. The geometry of components influences the location of stress concentration.

### 4.2.2 3D Von Mises Stress (MPa)

Table 4.2: Von Mises Stress in 3D Analysis

| | | Meshing Percentage | | | | |
|---|---|---|---|---|---|---|
| | | **100%** | **85%** | **75%** | **65%** | **50%** |
| Compression Ratio | 12 | 206.61 | 231.962 | **257.45** | 195.381 | 184.429 |
| | 12.5 | 197.559 | 199.086 | 211.766 | **263.826** | 199.299 |
| | 13 | 119.788 | 239.913 | **268.571** | 205.937 | 197.542 |
| | 13.5 | 236.173 | **251.305** | 238.67 | 213.7628 | 204.512 |
| | 14 | 258.261 | **258.2614** | 232.712 | 218.352 | 210.631 |
| | 14.5 | 238.807 | **257.808** | 218.982 | 215.693 | 214.0781 |
| | 15 | 242.141 | **260.937** | 217.129 | 225.372 | 223.636 |
| | 15.5 | 239.82 | **260.49** | 242.429 | 224.548 | 218.704 |
| | 16 | 242.436 | **256.662** | 242.434 | 223.174 | 227.429 |
| | 16.5 | **248.353** | 228.657 | 248.571 | 220.378 | 220.379 |
| | 17 | 221.822 | **230.123** | 217.125 | 223.563 | 213.429 |
| | **Average** | **222.8882** | **243.2004** | **235.9854** | **211.817** | **210.3698** |

From Table 4.2, meshing 85% is always shown the maximum value for Von Mises Stress and its average value is also higher than other meshing percentage in 3D analysis. For future analysis, the 85% is best to choose because it shows high value for Von Mises Stress. The higher value for each compression ratio value is picking up to generate new table as shown below. The new table is table 4.3.

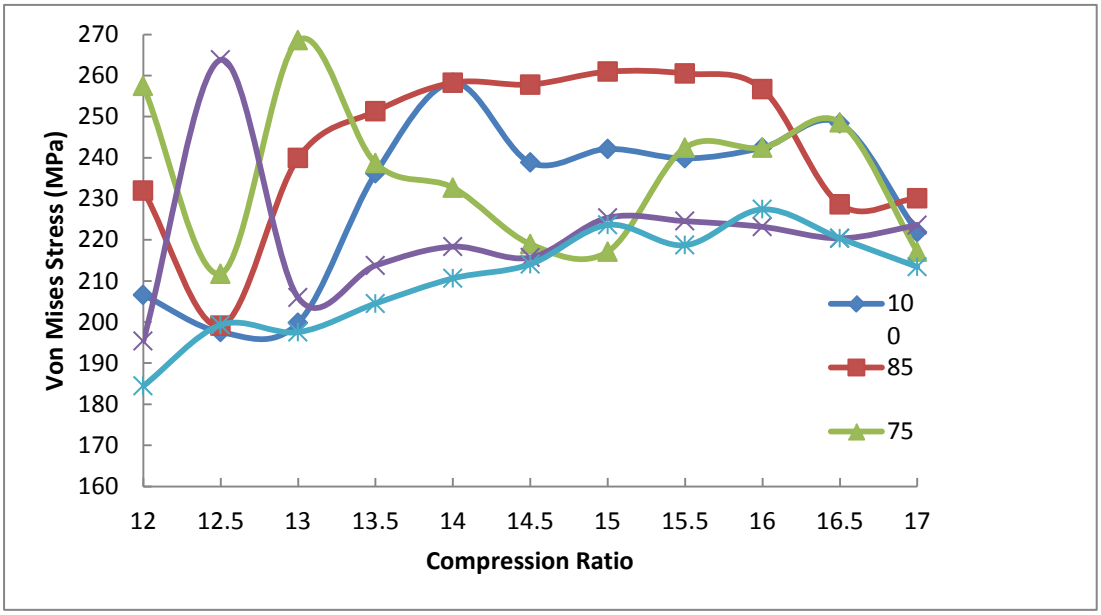


Figure 4.4: The effect of Von Mises Stress at different Compression Ratio

The Figure 4.4 is about Von Mises Stress Versus Compression Ratio. The Von Mises Stress patent value is getting converging when compression ratio increasing. For future analysis, meshing 85% and 75% is suitable for this model.

Table 4.3: Maximum Von Mises Stress in 3D Analysis

| Compression Ratio | | | | | | | | | | |
|---|---|---|---|---|---|---|---|---|---|---|
| 12 | 12.5 | 13 | 13.5 | 14 | 14.5 | 15 | 15.5 | 16 | 16.5 | 17 |
| Maximum Von Mises Stress (MPa) | | | | | | | | | | |
| 257.5 | 263.8 | 268.6 | 251.3 | 258.3 | 257.8 | 260.9 | 260.5 | 256.7 | 248.6 | 230.1 |

Each maximum value on Table 4.3 is picking up from Table 4.2 and produced the graph as shown below.

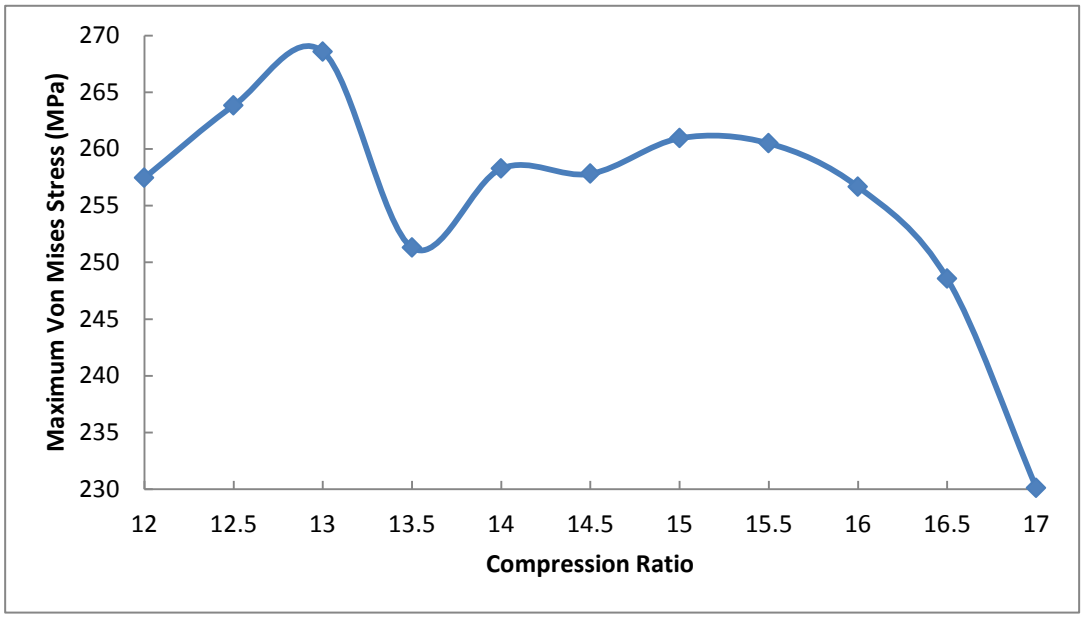


Figure 4.5: The effect of Maximum Von Mises Stress at different Compression Ratio

Figure above tell us about the higher value at compression ratio 13 and the magnitude value of Von Mises Stress is decreasing starting from compression ratio 15 until 17.

### 4.2.3 3D Maximum Principal Stress (MPa)

Table 4.4: Maximum Principal Stress in 3D Analysis

| | | Meshing Percentage | | | | |
|---|---|---|---|---|---|---|
| | | 100% | 85% | 75% | 65% | 50% |
| Compression Ratio | 12 | 142.115 | **189.16** | 153.752 | 130.067 | 158.439 |
| | 12.5 | 133.061 | 134.38 | **168.474** | 130.683 | 148.511 |
| | 13 | 155.243 | 140.063 | **171.496** | 141.293 | 151.466 |
| | 13.5 | 153.566 | 142.845 | 153.279 | 143.805 | **155.562** |
| | 14 | 148.412 | 152.826 | 160.183 | 150.096 | **161.468** |
| | 14.5 | **168.0511** | 166.583 | 152.488 | 192.74 | 164.55 |
| | 15 | 167.916 | 192.144 | **193.546** | 151.084 | 183.219 |
| | 15.5 | 167.981 | 156.926 | **195.535** | 153.976 | 168.807 |
| | 16 | 168.914 | 158.833 | 168.934 | 154.196 | **173.546** |
| | 16.5 | 161.706 | 140.253 | **182.3** | 154.879 | 155.686 |
| | 17 | 153.324 | **178.125** | 124.735 | 156.866 | 153.546 |
| | Average | 156.3899 | 159.2853 | 165.8838 | 150.8805 | 161.3455 |

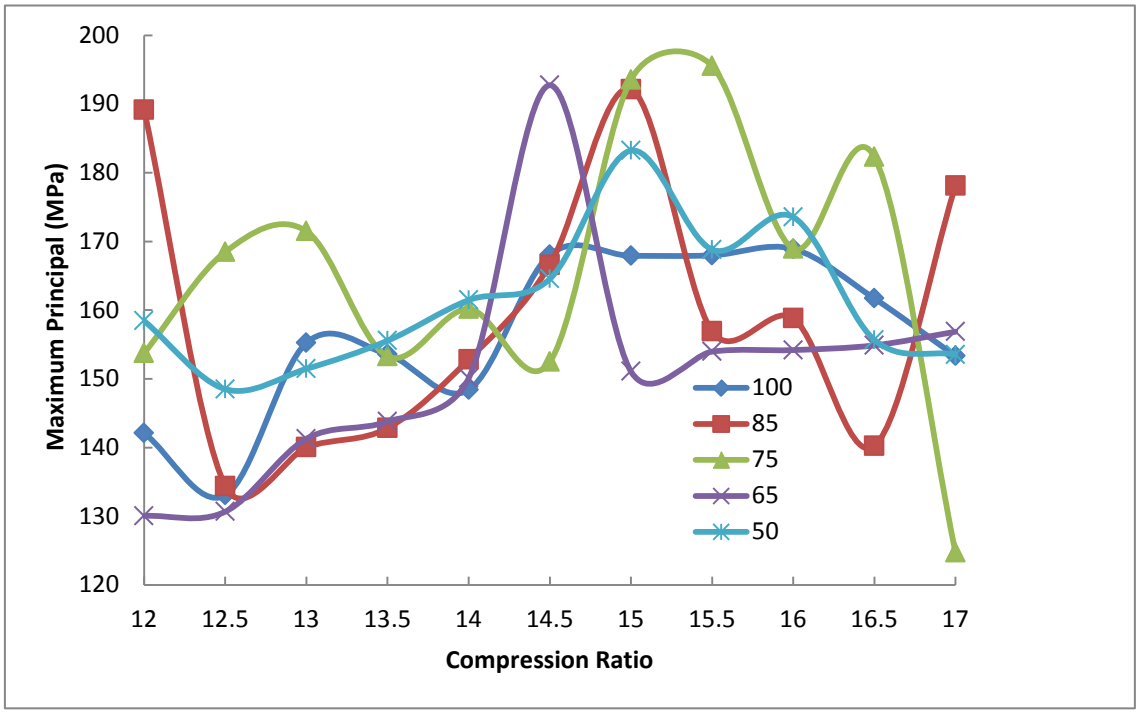


Figure 4.6: The effect of Maximum Principal Stress at different Compression Ratio

The graph above explained about patent of Maximum principal stress versus compression ratio. The maximum value for Maximum Principal Stress is about 196MPa at compression ratio 15.5. Its quite dificult to choose the best meshing percentage because the graph is to complicated.

Table 4.5: Maximum value for Maximum Principal Stress in 3D Analysis

| Compression Ratio | | | | | | | | | | |
|---|---|---|---|---|---|---|---|---|---|---|
| 12 | 12.5 | 13 | 13.5 | 14 | 14.5 | 15 | 15.5 | 16 | 16.5 | 17 |
| Maximum Principal Stress (MPa) | | | | | | | | | | |
| 189.2 | 168.5 | 171.5 | 155.6 | 161.5 | 168.1 | 193.6 | 195.5 | 173.6 | 182.3 | 178.1 |

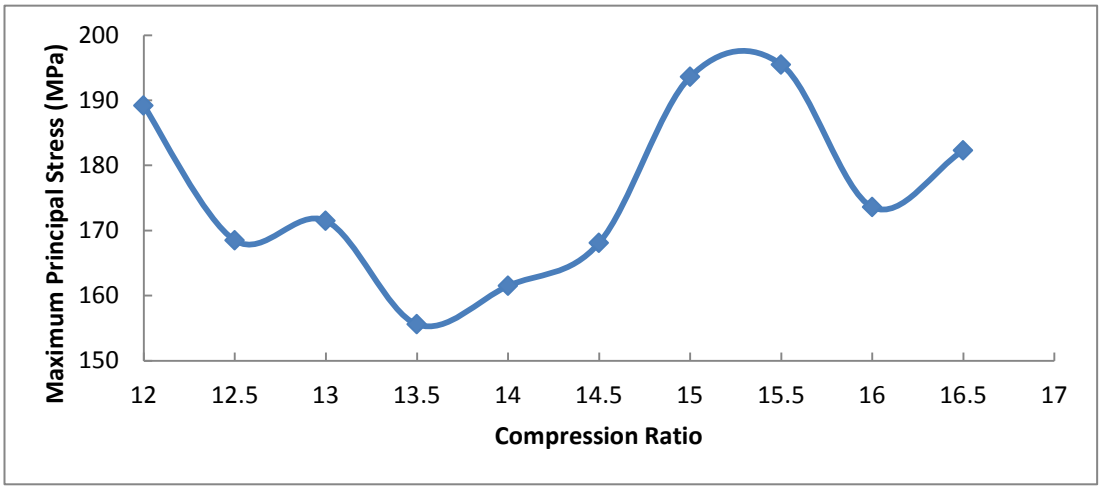


Figure 4.7: The effect of Maximum Principal Stress at different Compression Ratio

Figure above stated that the higher value for Maximum Principal Stress is about 196MPa at compression ratio 15.5. At compression ratio 14.5, the Maximum Principal Stress value is too low and it is suitable to use this piston in CNG engine.

### 4.2.4 3D Displacement Magnitude (mm)

Table 4.6: Displacement Magnitude in 3D Analysis

| | | Meshing Percentage | | | | |
|---|---|---|---|---|---|---|
| | | 100% | 85% | 75% | 65% | 50% |
| Compression Ratio | 12 | 0.12037 | 0.119115 | 0.120375 | 0.106592 | 0.120928 |
| | 12.5 | 0.11477 | 0.0904 | 0.114645 | 0.096074 | 0.117414 |
| | 13 | 0.110666 | 0.107385 | 0.116242 | 0.104905 | 0.115095 |
| | 13.5 | 0.120417 | 0.109281 | 0.10334 | 0.1069 | 0.110537 |
| | 14 | 0.109601 | 0.108065 | 0.118317 | 0.106439 | 0.109354 |
| | 14.5 | 0.121758 | 0.110146 | 0.106441 | 0.11556 | 0.11959 |
| | 15 | 0.115754 | 0.133091 | 0.115913 | 0.108513 | 0.109989 |
| | 15.5 | 0.115125 | 0.10511 | 0.11342 | 0.104148 | 0.108368 |
| | 16 | 0.11395 | 0.10366 | 0.11397 | 0.10263 | 0.10612 |
| | 16.5 | 0.12582 | 0.120767 | 0.12596 | 0.09888 | 0.09885 |
| | 17 | 0.110287 | 0.119149 | 0.112817 | 0.099255 | 0.09851 |

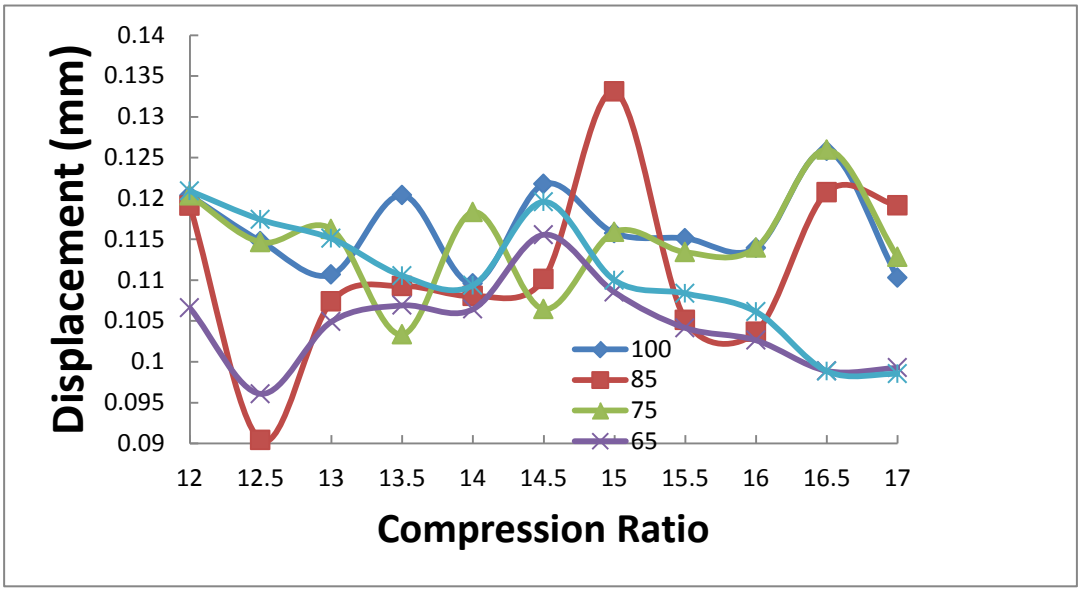


Figure 4.8: The effect of Displacement Magnitude at different Compression Ratio

Figure 4.8 explain about displecement magnitude versus compression ratio. The higher value for thr displacement magnitude is about 0.134mm at compression ratio 15 on the meshing of 85%. The maximum value dispacement magnitude for compression ratio at 14.5 is 0.122mm.

Table 4.7: Maximum value for Displacement Magnitude in 3D Analysis

| Compression Ratio | | | | | | | | | | |
|---|---|---|---|---|---|---|---|---|---|---|
| 12 | 12.5 | 13 | 13.5 | 14 | 14.5 | 15 | 15.5 | 16 | 16.5 | 17 |
| Maximum value for Displacement Magnitude (mm) | | | | | | | | | | |
| 0.1204 | 0.117 | 0.116 | 0.12 | 0.118 | 0.122 | 0.116 | 0.115 | 0.114 | 0.126 | 0.119 |

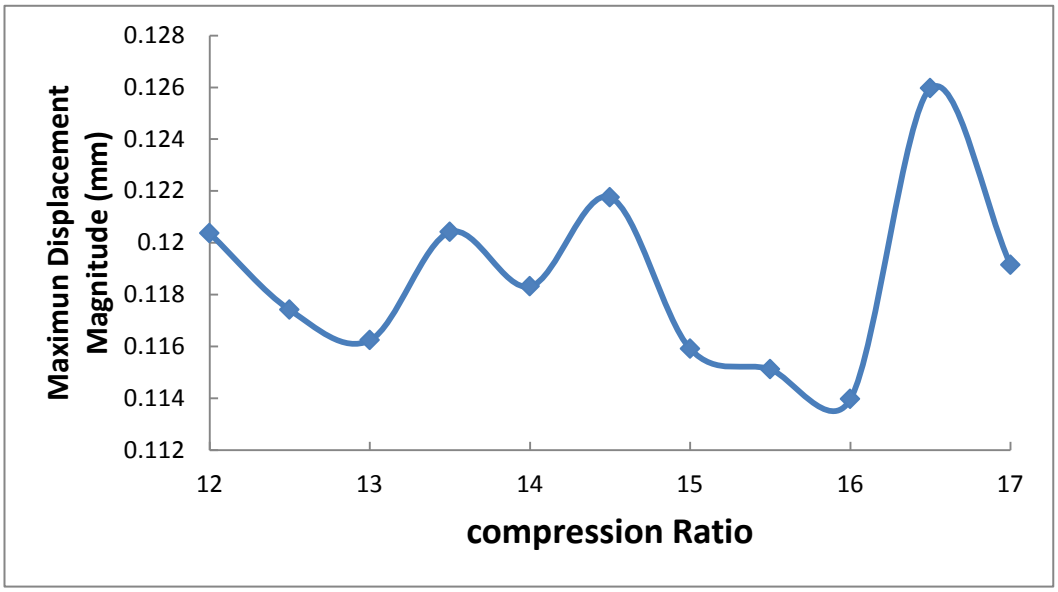


Figure 4.9: The effect of Maximum Displacement Magnitude at different Compression Ratio

Refer to Figure 4.9, the highest value for maximum dispacement is about 0.126mm and occur at compression ratio 16.5. At compression ratio 14.5, the displacement magnitude is about 0.122mm

### 4.2.5 3D Von Mises Strain (mm/mm)

Table 4.8: Strain in 3D Analysis

| | | Meshing Percentage | | | | |
|---|---|---|---|---|---|---|
| | | 100% | 85% | 75% | 65% | 50% |
| Compression Ratio | 12 | 0.003988 | 0.004478 | 0.00497 | 0.00377 | 0.00356 |
| | 12.5 | 0.003814 | 0.003843 | 0.004088 | 0.003162 | 0.003847 |
| | 13 | 0.003857 | 0.00463 | 0.005184 | 0.003975 | 0.003813 |
| | 13.5 | 0.004559 | 0.00485 | 0.004607 | 0.004126 | 0.003947 |
| | 14 | 0.00499 | 0.004631 | 0.00449 | 0.00421 | 0.00407 |
| | 14.5 | 0.00461 | 0.00498 | 0.00423 | 0.00416 | 0.00413 |
| | 15 | 0.00467 | 0.005037 | 0.00419 | 0.00435 | 0.00444 |
| | 15.5 | 0.004629 | 0.005028 | 0.00468 | 0.004335 | 0.004221 |
| | 16 | 0.00468 | 0.00495 | 0.00468 | 0.004308 | 0.004 |
| | 16.5 | 0.00479 | 0.004414 | 0.004798 | 0.004252 | 0.004254 |
| | 17 | 0.004282 | 0.00444 | 0.00419 | 0.004315 | 0.004151 |

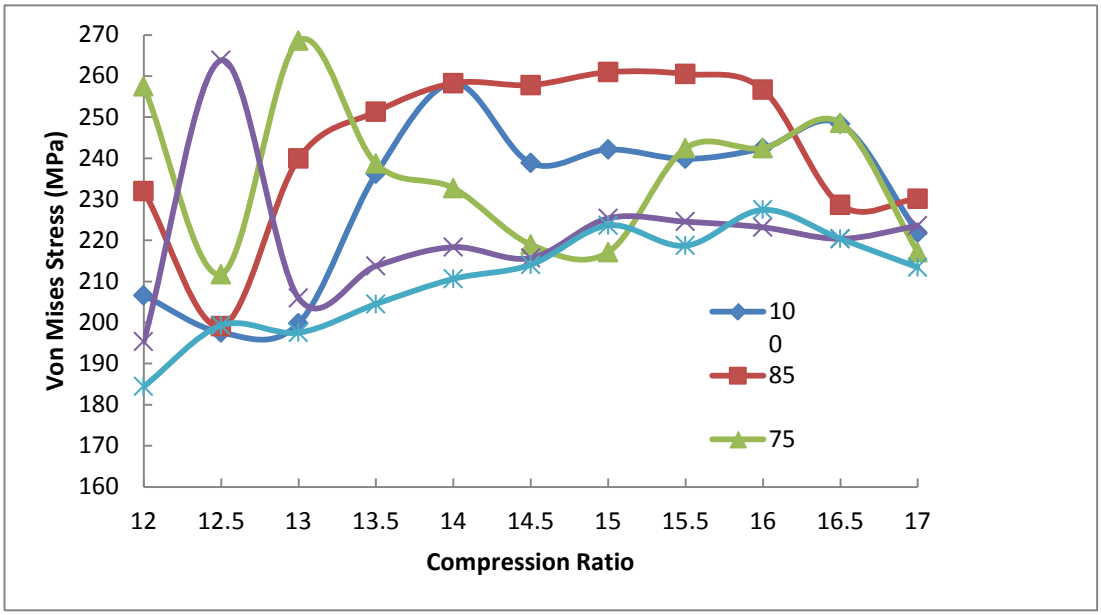


Figure 4.10: The effect of Strain at different Compression Ratio

Figure above explain about strain versus compression ratio. The highest value is about 0.0052mm/mm at compression ratio 13 on meshing 75%. For compressio ratio 14.5, the maximum strain value is about 0.005mm/mm on meshing 100%.

Table 4.9: Maximum Strain in 3D Analysis

| Compression Ratio | | | | | | | | | | |
|---|---|---|---|---|---|---|---|---|---|---|
| 12 | 12.5 | 13 | 13.5 | 14 | 14.5 | 15 | 15.5 | 16 | 16.5 | 17 |
| Maximum value for Strain (mm/mm) | | | | | | | | | | |
| 0.005 | 0.004 | 0.005 | 0.005 | 0.005 | 0.005 | 0.005 | 0.005 | 0.005 | 0.005 | 0.004 |

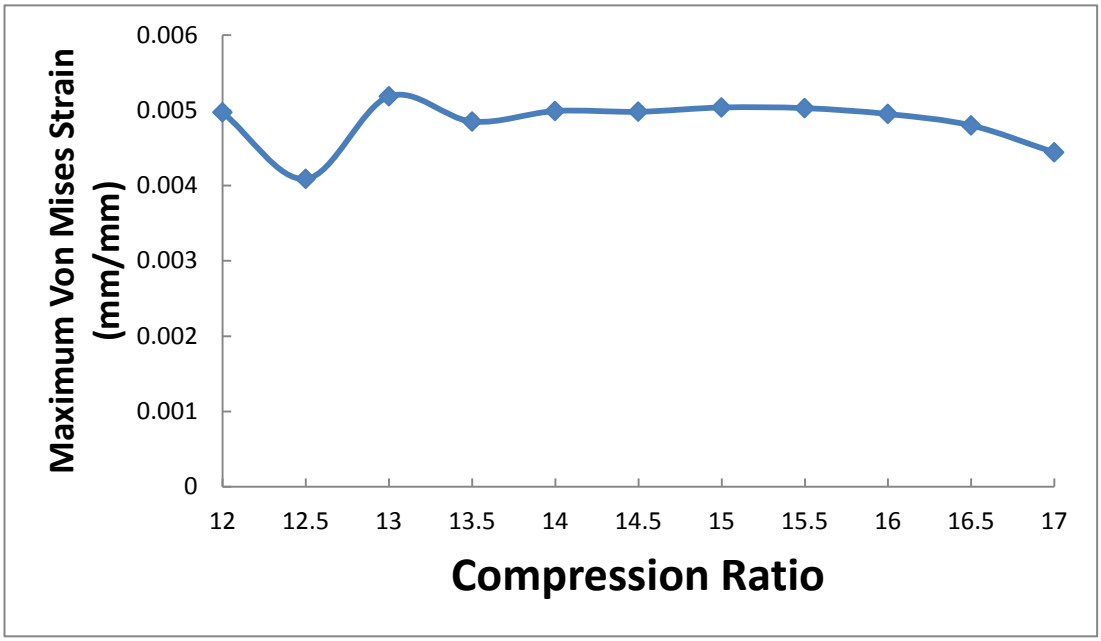


Figure 4.11: The effect of Maximum Von Mises Strain at different Compression Ratio

Figure as shown above explained that at compression ratio 12 until 17, the value for strain is constant. At compression ratio 14.5, the maximum Von Mises Strain is about 0.005mm/mm.

## 4.3 PRESSURE-2D ANALYSIS

### 4.3.1 2D Maximum Von Mises Stress (MPa)

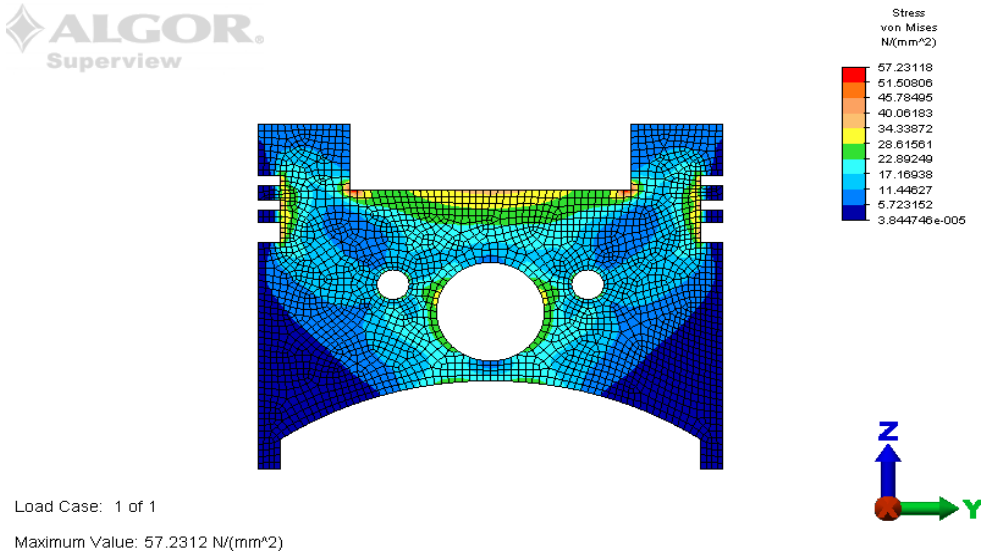

Figure 4.12: Von Mises Stress at Compression Ratio 14.5 and meshing Density 4000.

Table 4.10: Von Mises Stress (MPa) in 2D analysis

| Compression Ratio | Meshing Density | | | | | | | |
|---|---|---|---|---|---|---|---|---|
| | 500 | 1000 | 1500 | 2000 | 2500 | 3000 | 3500 | 4000 |
| 12.0 | 77.5769 | 79.0263 | 79.0915 | 79.1753 | 80.2187 | 80.4748 | **80.56** | 77.3416 |
| 12.5 | 75.2595 | 76.2205 | 76.3437 | 76.8105 | 77.0891 | 77.5949 | **77.8887** | 74.5289 |
| 13.0 | 62.6225 | 64.8616 | 64.8031 | 66.1132 | 66.1696 | 66.2297 | **66.4639** | 65.6799 |
| 13.5 | 60.0286 | 60.0387 | 61.0669 | 61.317 | 61.4247 | 61.6085 | **62.0197** | 61.9326 |
| 14.0 | 56.0944 | 56.1458 | 57.9698 | 57.9907 | 58.054 | 58.0431 | 58.5444 | **59.9139** |
| 14.5 | 52.9784 | 54.6823 | 54.844 | 54.6025 | 54.6609 | 54.9442 | 56.5607 | **57.2312** |
| 15.0 | 50.3281 | 52.1654 | 52.3011 | 52.2172 | 52.83 | 53.6528 | 53.7324 | **56.576** |
| 15.5 | 49.1312 | 49.7213 | 50.0489 | 50.1096 | 50.3008 | 52.5971 | 53.7016 | **55.0396** |
| 16.0 | 47.0545 | 47.0843 | 48.0843 | 48.6977 | 49.5093 | 50.4404 | 52.9318 | **54.5926** |
| 16.5 | 45.441 | 46.4862 | 46.6419 | 46.9488 | 49.0632 | 50.9529 | 51.8149 | **52.7318** |
| 17.0 | 44.9888 | 45.0371 | 45.5534 | 46.355 | 47.355 | 50.3502 | 51.2747 | **52.7451** |

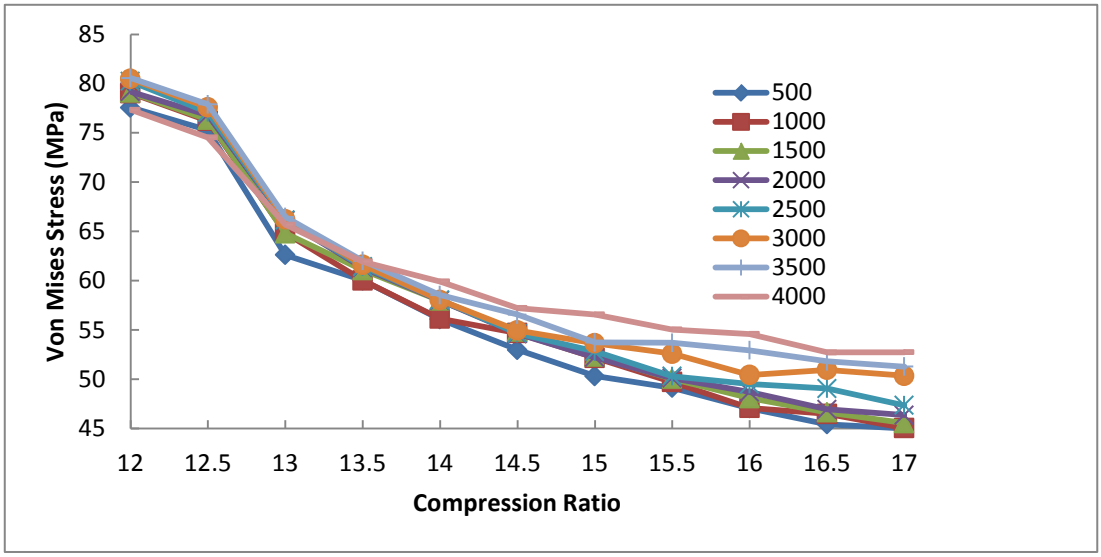


Figure 4.13: The effect of Von Mises Stress at different Compression Ratio

Table 4.11: Maximum Von Mises Stress (MPa) in 2D analysis

| Compression Ratio | | | | | | | | | | |
|---|---|---|---|---|---|---|---|---|---|---|
| 12 | 12.5 | 13 | 13.5 | 14 | 14.5 | 15 | 15.5 | 16 | 16.5 | 17 |
| Maximum Von Mises Stress (MPa) | | | | | | | | | | |
| 80.6 | 77.9 | 66.5 | 62 | 59.9 | 57.2 | 56.6 | 55 | 54.6 | 53 | 52.8 |

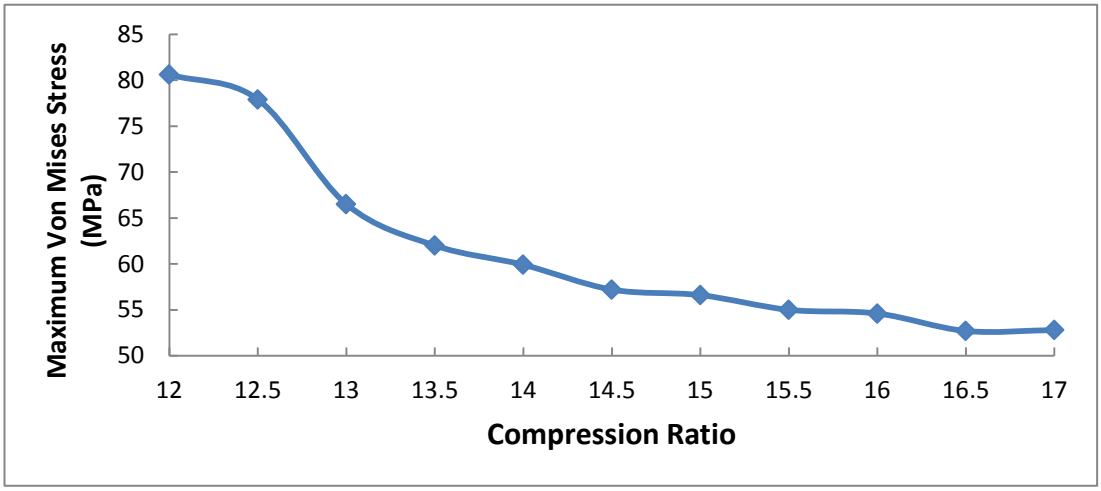


Figure 4.14: The effect of Maximum Von Mises Stress at different Compression Ratio

The piston remains in shape and no deformation is approximately occurring that lead to failure of the piston during normal operation of the engine if the compression ratio is at 14.5.

### 4.3.2 2D Maximum Principal Stress (MPa)

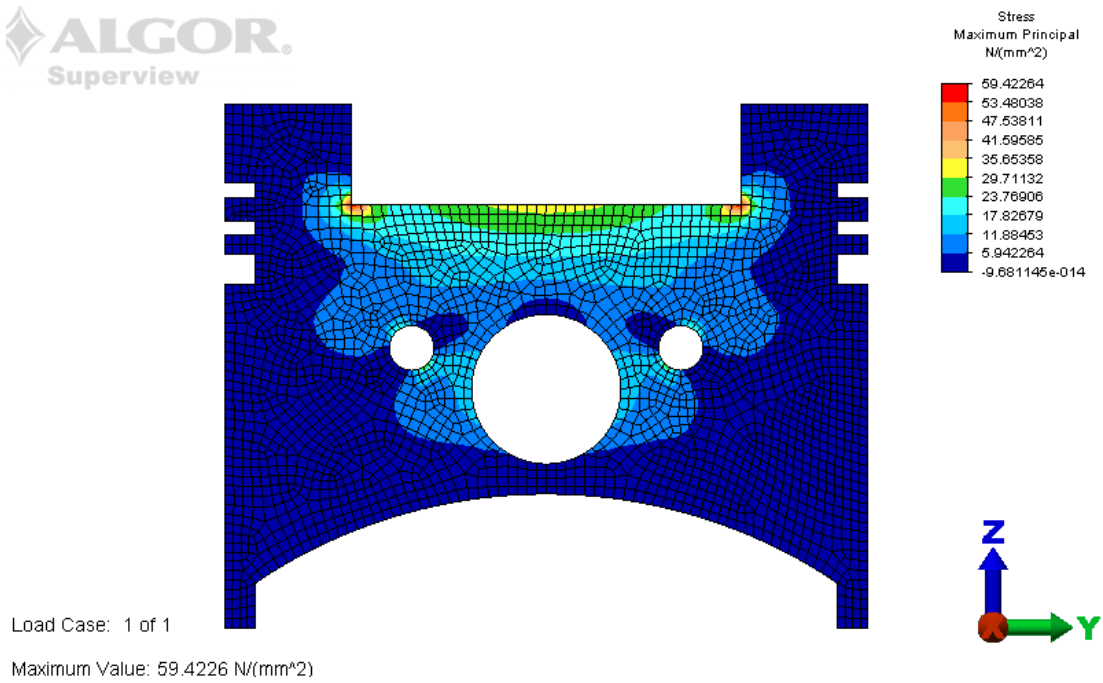


Figure 4.15: Maximum Principal Stress at Compression Ratio 14.5 and meshing density 4000.

Table 4.12: Maximum Principal Stress (MPa) in 2D Analysis

Table 4.13: Stress Maximum principal in 2D analysis

| Compression Ratio | Meshing Density | | | | | | | |
|---|---|---|---|---|---|---|---|---|
| | 500 | 1000 | 1500 | 2000 | 2500 | 3000 | 3500 | 4000 |
| 12.0 | 48.0994 | 57.0315 | 59.8352 | 68.5865 | 70.2784 | 78.732 | 78.4633 | 79.6085 |
| 12.5 | 47.687 | 55.7339 | 58.1267 | 67.4486 | 68.6315 | 75.4982 | 76.5871 | 77.4071 |
| 13.0 | 45.4645 | 49.5369 | 51.3538 | 58.6272 | 59.6809 | 67.7828 | 66.9206 | 68.5272 |
| 13.5 | 43.2966 | 47.0715 | 51.8318 | 55.762 | 57.0308 | 63.5033 | 63.7772 | 63.8887 |
| 14.0 | 40.9243 | 45.0194 | 47.208 | 52.9734 | 53.965 | 59.4821 | 59.7188 | 62.1966 |
| 14.5 | 39.9901 | 42.6546 | 43.4785 | 50.9438 | 51.3684 | 56.0022 | 56.2561 | 59.4226 |
| 15.0 | 39.8914 | 41.2779 | 41.9591 | 49.2439 | 49.6924 | 53.9723 | 55.5422 | 57.1165 |
| 15.5 | 39.9719 | 39.74 | 41.6107 | 47.651 | 48.4645 | 52.3363 | 53.7961 | 54.0324 |
| 16.0 | 37.7317 | 38.7151 | 41.1608 | 45.2072 | 46.6192 | 51.0884 | 50.517 | 53.0277 |
| 16.5 | 37.8243 | 38.4975 | 39.8281 | 44.3052 | 45.8589 | 50.2377 | 49.3069 | 50.6054 |
| 17.0 | 37.7396 | 37.2122 | 39.4486 | 43.5843 | 44.3694 | 48.0522 | 48.3212 | 50.2763 |

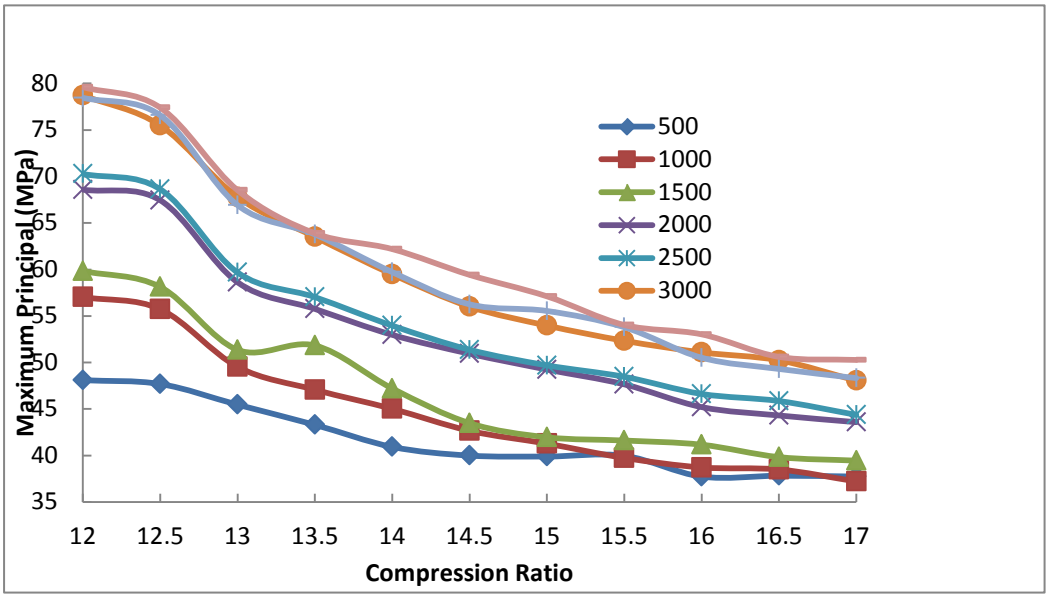


Figure 4.16: The effect of Maximum Principal Stress at different Compression Ratio

Table 4.13: Maximum value of Maximum Principal Stress (MPa) in 2D analysis

| Compression Ratio | | | | | | | | | | |
|---|---|---|---|---|---|---|---|---|---|---|
| 12 | 12.5 | 13 | 13.5 | 14 | 14.5 | 15 | 15.5 | 16 | 16.5 | 17 |
| Maximum Von Mises Stress (MPa) | | | | | | | | | | |
| 79.6 | 77.4 | 68.5 | 63.9 | 62.2 | 59.4 | 57.1 | 54 | 53 | 50.6 | 50.3 |

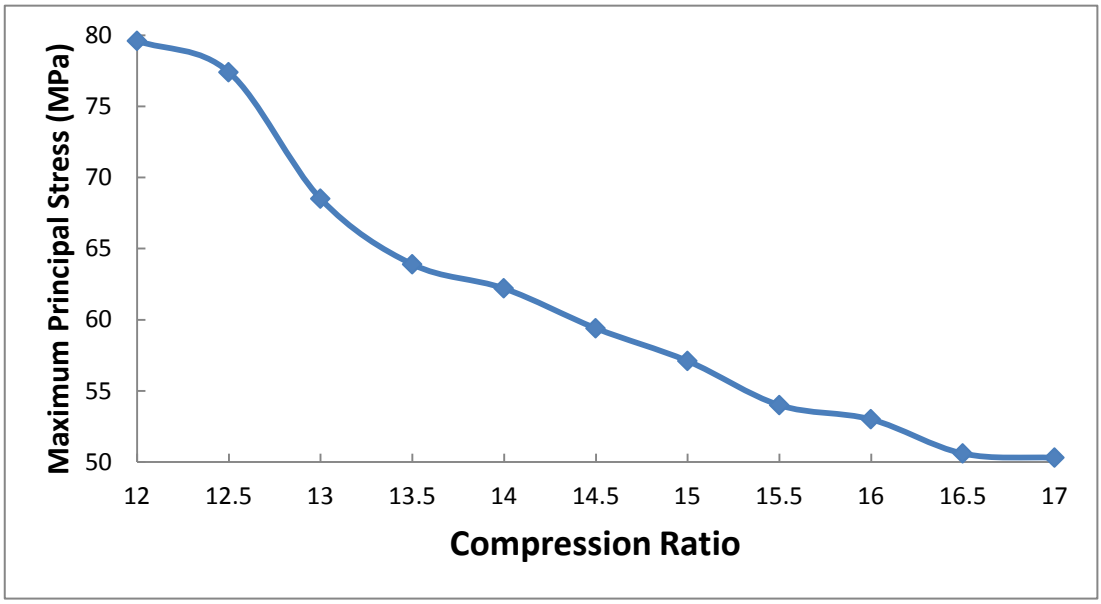


Figure 4.17: The effect of Maximum Principal Stress at different Compression Ratio

### 4.3.3 2D Stress Tensor Y-Y (MPa)

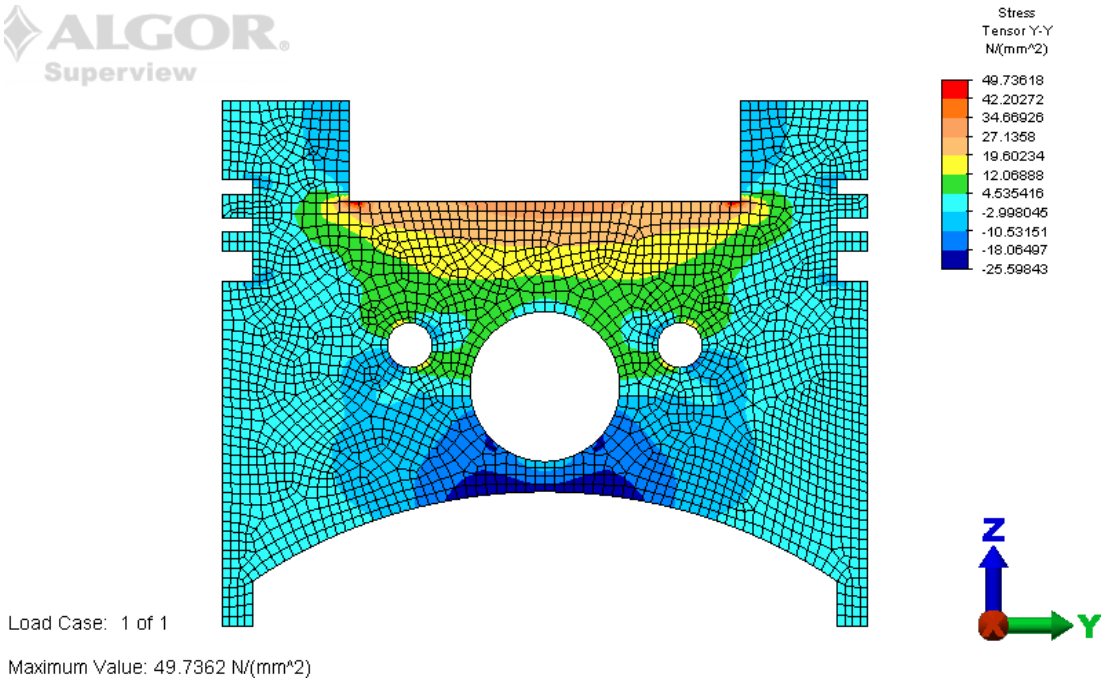


Figure 4.18: Maximum Stress Tensor Y-Y at Compression Ratio 14.5 and Meshing Density 4000

Table 4.14: Stress Tensor Y-Y in 2D analysis

| Compression Ratio | Meshing Density | | | | | | | |
|---|---|---|---|---|---|---|---|---|
| | 500 | 1000 | 1500 | 2000 | 2500 | 3000 | 3500 | 4000 |
| 12.0 | 46.4865 | 46.2061 | 50.5015 | 53.5003 | 56.4878 | 58.8542 | 60.5756 | 64.3007 |
| 12.5 | 46.0369 | 45.5243 | 50.0758 | 52.608 | 55.8671 | 56.803 | 59.8457 | 61.0511 |
| 13.0 | 42.6685 | 41.9414 | 44.7216 | 47.736 | 50.4952 | 52.5377 | 54.3214 | 57.1783 |
| 13.5 | 41.7766 | 41.0193 | 43.3307 | 45.8042 | 49.3307 | 49.9536 | 53.2328 | 53.8719 |
| 14.0 | 39.4257 | 40.3982 | 42.559 | 45.0041 | 47.0099 | 49.2812 | 49.8717 | 51.9125 |
| 14.5 | 38.9053 | 38.3256 | 40.8787 | 42.9803 | 45.348 | 46.6731 | 48.9942 | 49.7362 |
| 15.0 | 38.7861 | 37.9434 | 40.5329 | 42.4701 | 45.178 | 46.3345 | 46.7563 | 49.2335 |
| 15.5 | 38.7973 | 37.9649 | 40.1085 | 42.1582 | 43.0141 | 45.5252 | 46.7575 | 47.9245 |
| 16.0 | 36.9491 | 37.5245 | 39.8794 | 40.6595 | 43.0994 | 44.4404 | 46.0353 | 47.6374 |
| 16.5 | 37.054 | 37.4862 | 38.6646 | 40.5845 | 42.1912 | 44.3394 | 45.0625 | 46.1177 |
| 17.0 | 36.9453 | 36.2313 | 38.3763 | 40.1882 | 41.6728 | 43.642 | 44.6453 | 46.1976 |

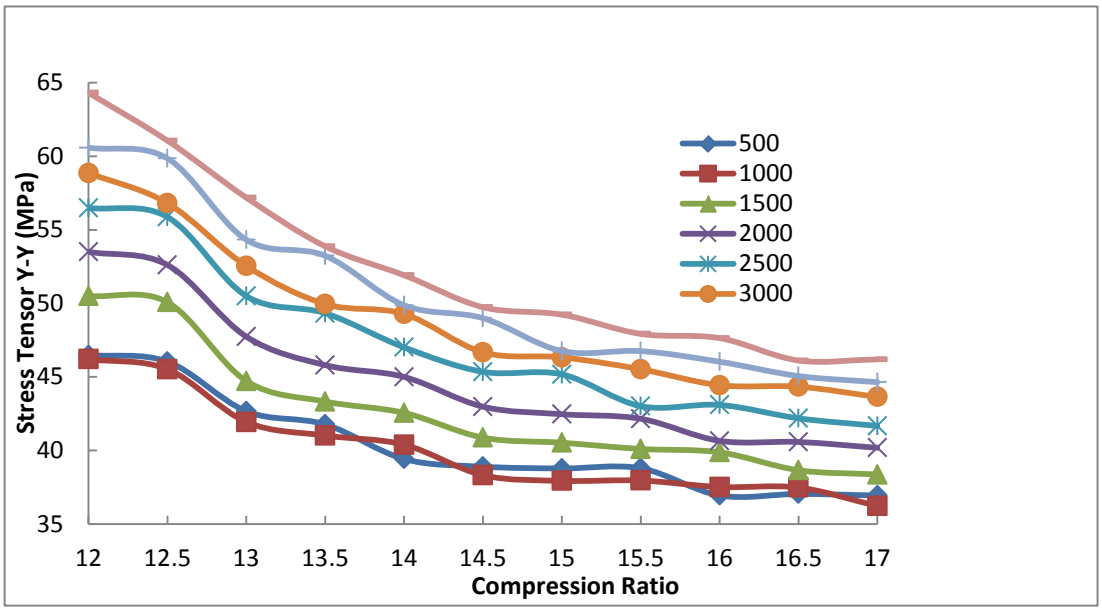


Figure 4.19: The effect of Stress Tensor Y-Y at different Compression Ratio

Table 4.15: Maximum Stress Tensor Y-Y in 2D analysis

| Compression Ratio | | | | | | | | | | |
|---|---|---|---|---|---|---|---|---|---|---|
| 12 | 12.5 | 13 | 13.5 | 14 | 14.5 | 15 | 15.5 | 16 | 16.5 | 17 |
| Maximum Von Mises Stress (MPa) | | | | | | | | | | |
| 64.3 | 61.1 | 57.2 | 53.9 | 51.9 | 49.7 | 49.2 | 47.9 | 47.6 | 46.1 | 46.2 |

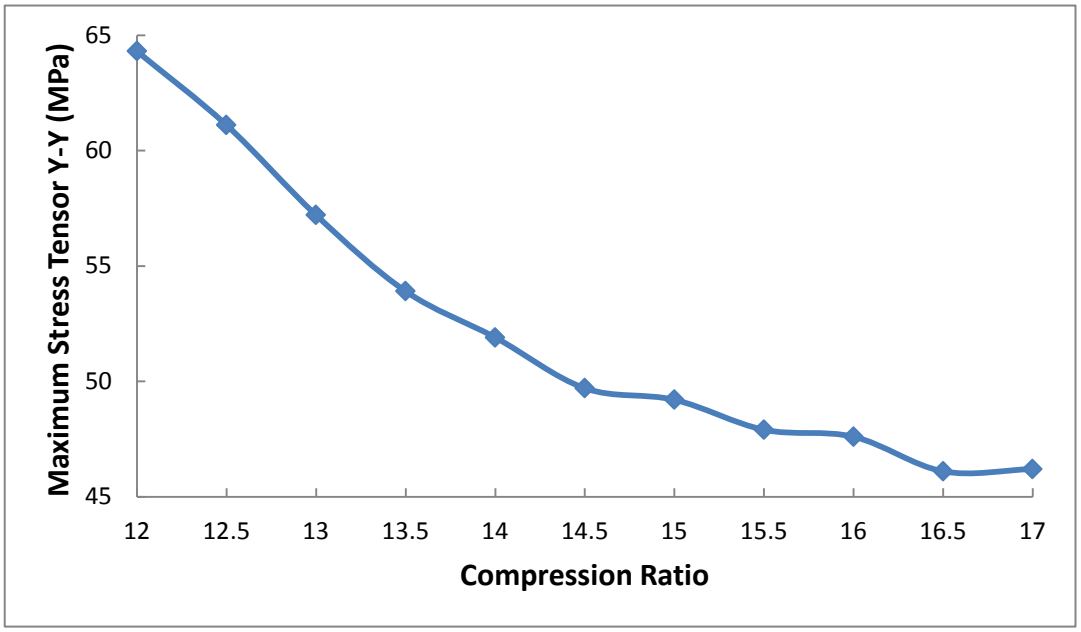


Figure 4.20: The effect of Maximum Stress Tensor Y-Y at different Compression Ratio

## 4.4 Problems and Errors

Problems occur while designing the component. All the components have complex shape and require lot of time to design. More over, the measurement are taken using vernier caliper and error can occur. CMM machine using Calypso software in FKM lab has difficulty to scan small holes at piston.

In order to analyze using static mode, the computer must have sufficient memory and high processor. The literature of analysis is limited to the piston. More over, the sources from the internet are suspicious about the contents. The result obtained from the analysis is incomparable to other previous research.

# CHAPTER 5

# CONCLUSION

## 5.1 Overall Conclusion

The first main conclusion that could be drawn from this work is that although fatigue is not responsible for biggest slice of damaged pistons, it remains a problem on engine pistons and its solution remains a goal for piston manufacturers. The problem will last for long because efforts on fuel consumption reduction and power increase will push to the limit in weight reduction that means thinner walls and higher stresses. To satisfy all the requirements with regards to successful application of pistons, in particular mechanical and high temperature mechanical fatigue and thermal/thermal–mechanical fatigue. There are several concepts available that can be used to improve its use, such as design, materials, processing technologies, etc

For the determination of stress concentration, the analysis is done by using Algor software. Static mode is use to approximately locate the maximum stress concentration. Since the analysis is done without any lubricant, wear is clearly occurred at the piston. The piston is approximately not to fail if compression ratio 14.5 is chosen. The reason is the piston approximately remains in shape since the maximum stress value is not more than the allowable stress of the materials. From the finite element analysis, high stresses occur at the structural member contains a discontinuity such as a holes or sudden change in cross section area.

If the piston can withstand the pressure and temperature effect, the alternative fuel to the petroleum can be solved. Besides that, the size of mesh will affect the result. For 3D analysis, the right meshing is meshing 75% and 85%. For 2D analysis, the higher

meshing density is required for examples meshing density higher than 4000. It is because the selection of appropriate mesh will give the best result.

## 5.2 Future Recommendation

Future analysis is recommended to include heat transfer to the system and destructive test while considering the lubricant on the system. For future analysis, focus only on 3D analysis. On 3D analysis, various shapes of bowl and different materials are to be analyse.

About the design of piston, two specific areas that are under high stresses need an improvement in design: the bowl rim area and the pin bore area. In addition, a larger bowl diameter and reduced bowl depth improved piston strength significantly. Thermal fatigue cracks and high temperature mechanical fatigue cracks may be reduced with design improvement.

The development of new materials and processing technologies with improved high temperature mechanical and fatigue performance would help to solve the different fatigue damages identified in this work.

Two specific areas that are under high stresses need an improvement in design: the bowl rim area and the pin bore area. Sharp edges or small radii on the bowl rim induce locally steeper temperature gradients and an increased stress of the material. In addition, a larger bowl diameter and reduced bowl depth improve piston strength significantly. Thermal fatigue cracks and high temperature mechanical fatigue cracks may be reduced with design improvemen

Another possible future development may include hard anodizing of the piston crown, in diesel pistons; to prevent thermal fatigue crack initiation. This treatment by reducing friction would be useful to reduce wear at the cylinder wall. This means that clearances would resist more time and problems such as broken grooves and broken skirts would be avoided.

# REFERENCES


[1]. Ibrahim, N.M.I.N; Ismail, A; Rahim, M.F; Bakar, R.A and Rahman, M.R. Visualization of the scavenging process two-stroke spark ignition engine using CFD. *Universiti Malaysia Pahang.*

[2]. Dixon, M.P. 2002. Internal combustion engine with variable compression ratio. *US Patent 6427643.*

[3]. Cengel, Y.A. and Boles, M.A. 2006. Thermodynamics: An engineering approach. *The McGraw Hill Companies.*

[4]. Kobayashi, T; Nakamura, N; Nomura, K; Nomura, H; Nihei, H and Ohno, E. 1995. A two stroke engine. *Patent Lens EP 463613 B1.*

[5]. Greenman, M.D. 1996. Design and construction of a miniature internal combustion engine. *Massachusetts Institute of Technology.*

[6]. Ke Zeng, Zuohua Huang. Combustion characteristics of a direct-injection natural gas engine under various fuel injection timings. *Applied Thermal Engineering 26 (2006) 806–813.*

[7]. S. Zhang and a. Sobiesiak. The first and second law analyses of a port-injected, spark ignition engine fuelled with compressed natural gas. *Department of mechanical, automotive and materials engineering university of Windsor, Canada.*

[8]. von Mises, R. (1913). *Mechanik der Festen Korper im plastisch deformablen Zustand.* Göttin. Nachr. Math. Phys., vol. 1, pp. 582–592.

[9]. David J Grieve, Piston Analysis: 27th October 2006

[10]. Junker H, Issler W. Pistons for high loaded direct injection diesel engines. MAHLE Technical Information.

[11]. C.M. Taylo, Automobile engine tribology – design considerations for efficiency and durability, *Wear* **221** (1998), pp. 1–8.

[12]. H. Kajiwara, Y. Fujioka, T. Suzuki and H. Negishi, An analytical approach for prediction of piston temperature distribution in diesel engines, *JSAE Rev* **23** (2002)

[13]. F. Payri, J. Benajes, X. Margot and A. Gil, CFD modeling of the in-cylinder flow in direct-injection diesel engines, *Comput Fluids* **33** (2004)

[14]. **F.S. Silva.** Fatigue on engine pistons – A compendium of case studies. Department of Mechanical Engineering, University of Minho, Azurém. December 2004

[15]. Dr. F. Atzler. On the Future of the Piston Engine with Internal Combustion. Marie Curie Fellowship Conference Wednesday of May 2001.

[16]. MAHLE, Kolben fur Verbrennungsmotoren Die Bibliothek der Technik; 1998. p. 39.

[17]. M.R. Joyce, C.M. Styles and P.A.S. Reed, Elevated temperature short crack fatigue behaviour in near eutectic Al–Si alloys, *Int J Fatigue* **25** (2003), pp. 863–869.

[18]. MAHLE, Pistons for high loaded direct injection diesel engines. Technical Information. p. 12.

[19]. John B. Heywood. Internal Combustion Engine Fundamentals. McGRAW-HILL. Automotive Technology Series.